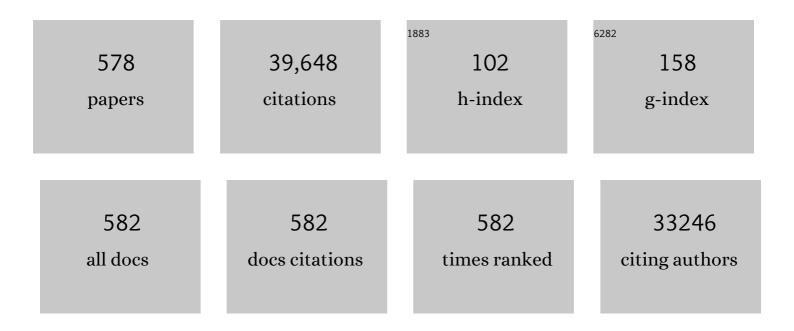


List of Publications by Year in descending order

Source: https://exaly.com/author-pdf/8657799/publications.pdf Version: 2024-02-01



Χιε ΟιιαΝ

#	Article	IF	CITATIONS
1	Electroconductive RGO-MXene membranes with wettability-regulated channels: improved water permeability and electro-enhanced rejection performance. Frontiers of Environmental Science and Engineering, 2023, 17, .	3.3	12
2	Multiple application of SAzyme based on carbon nitride nanorod-supported Pt single-atom for H2O2 detection, antibiotic detection and antibacterial therapy. Chemical Engineering Journal, 2022, 427, 131572.	6.6	42
3	Enhancing anoxic denitrification of low C/N ratio wastewater with novel ZVI composite carriers. Journal of Environmental Sciences, 2022, 112, 180-191.	3.2	23
4	Enhanced degradation of organic water pollutants by photocatalytic in-situ activation of sulfate based on Z-scheme g-C3N4/BiPO4. Chemical Engineering Journal, 2022, 428, 132116.	6.6	48
5	Accelerating anaerobic hydrolysis acidification of dairy wastewater in integrated floating-film and activated sludge (IFFAS) by using zero-valent iron (ZVI) composite carriers. Biochemical Engineering Journal, 2022, 177, 108226.	1.8	26
6	Treatment of organic wastewater by a synergic electrocatalysis process with Ti3+ self-doped TiO2 nanotube arrays electrode as both cathode and anode. Journal of Hazardous Materials, 2022, 424, 127747.	6.5	22
7	Robust ultrathin nanoporous MOF membrane with intra-crystalline defects for fast water transport. Nature Communications, 2022, 13, 266.	5.8	76
8	Electro-Fenton improving fouling mitigation and microalgae harvesting performance in a novel membrane photobioreactor. Water Research, 2022, 210, 117955.	5.3	10
9	Enhancing the formation of simultaneous nitriï¬cation and denitriï¬cation (SND) biofilm and nitrogen removal performance using two-units IFFAS process filled with surface-modified carriers. Biochemical Engineering Journal, 2022, 179, 108316.	1.8	9
10	Design Principles and Strategies of Photocatalytic H ₂ O ₂ Production from O ₂ Reduction. ACS ES&T Engineering, 2022, 2, 1068-1079.	3.7	51
11	Fabrication of FeOCI nanoparticles modified microchannel carbon cathode for flow-through electro-Fenton degradation of refractory organic pollutants. Separation and Purification Technology, 2022, 288, 120661.	3.9	23
12	Synergistic induced charge transfer switch by oxygen vacancy and pyrrolic nitrogen in MnFe2O4/g-C3N4 heterojunctions for efficient transformation of bicarbonate to acetate in photo-assisted MES. Applied Catalysis B: Environmental, 2022, 307, 121214.	10.8	35
13	Enhancing anaerobic methane production in integrated floating-film activated sludge system filled with novel MWCNTs-modified carriers. Chemosphere, 2022, 299, 134483.	4.2	6
14	Non-doping 3D porous carbon with rich intrinsic defects for efficient nonradical activation of peroxymonosulfate toward the degradation of organic pollutants. Separation and Purification Technology, 2022, 292, 121048.	3.9	19
15	High-efficiency electrochemical activation of H2O2 into ·OH enabled by flow-through FeOCl-modified carbon electrode for organic pollutants degradation. Separation and Purification Technology, 2022, 295, 121279.	3.9	6
16	Selective molecular separation with conductive MXene/CNT nanofiltration membranes under electrochemical assistance. Journal of Membrane Science, 2022, 658, 120719.	4.1	26
17	Electro-assisted CNTs/ceramic flat sheet ultrafiltration membrane for enhanced antifouling and separation performance. Frontiers of Environmental Science and Engineering, 2021, 15, 1.	3.3	27
18	Operating redox couple transport mechanism for enhancing photocatalytic H2 generation of Pt and CrOx-decorated ZnCdS nanocrystals. Applied Catalysis B: Environmental, 2021, 283, 119601.	10.8	44

#	Article	lF	CITATIONS
19	Degradation of aqueous bisphenol A in the CoCN/Vis/PMS system: Catalyst design, reaction kinetic and mechanism analysis. Chemical Engineering Journal, 2021, 407, 127228.	6.6	68
20	Photocatalytic ozonation of organic pollutants in wastewater using a flowing through reactor. Journal of Hazardous Materials, 2021, 405, 124277.	6.5	24
21	Efficient production of acetate from inorganic carbon (HCO3–) in microbial electrosynthesis systems incorporating Ag3PO4/g-C3N4 anaerobic photo-assisted biocathodes. Applied Catalysis B: Environmental, 2021, 284, 119696.	10.8	37
22	Carbon-Based Materials for Electrochemical Reduction of CO ₂ to C ₂₊ Oxygenates: Recent Progress and Remaining Challenges. ACS Catalysis, 2021, 11, 2076-2097.	5.5	116
23	Efficient Light-Driven Fuel Cell with Simultaneous Degradation of Pollutants on a TiO ₂ Photoanode and Production of H ₂ O ₂ on a Gas Diffusion Electrode Cathode. ACS ES&T Engineering, 2021, 1, 1122-1130.	3.7	11
24	A porous carbon-based electro-Fenton hollow fiber membrane with good antifouling property for microalgae harvesting. Journal of Membrane Science, 2021, 626, 119189.	4.1	26
25	Efficient electrochemical nitrate removal on Cu and nitrogen doped carbon. Chemical Engineering Journal, 2021, 415, 128958.	6.6	36
26	Highly efficient metal-free electro-Fenton degradation of organic contaminants on a bifunctional catalyst. Journal of Hazardous Materials, 2021, 416, 125859.	6.5	49
27	Alternating current-enhanced carbon nanotubes hollow fiber membranes for membrane fouling control in novel membrane bioreactors. Chemosphere, 2021, 277, 130240.	4.2	12
28	Enhancing the treatment of petrochemical wastewater using redox mediator suspended biofilm carriers. Biochemical Engineering Journal, 2021, 173, 108087.	1.8	10
29	Flow-through heterogeneous electro-Fenton system based on the absorbent cotton derived bulk electrode for refractory organic pollutants treatment. Separation and Purification Technology, 2021, 276, 119266.	3.9	30
30	Selective reduction of nitrate to ammonium over charcoal electrode derived from natural wood. Chemosphere, 2021, 285, 131501.	4.2	16
31	Computer Assisted Design of Electro-Fenton Reactor to Improve the Pollutants Degradation Ability. Journal of Physics: Conference Series, 2021, 2033, 012062.	0.3	0
32	Enhanced Chlorinated Pollutant Degradation by the Synergistic Effect between Dechlorination and Hydroxyl Radical Oxidation on a Bimetallic Single-Atom Catalyst. Environmental Science & Technology, 2021, 55, 14194-14203.	4.6	70
33	Simultaneous Heteroatom Doping and Microstructure Construction by Solid Thermal Melting Method for Enhancing Photoelectrochemical Property of g-C3N4 Electrodes. Separation and Purification Technology, 2021, , 120005.	3.9	7
34	Durable and Selective Electrochemical H ₂ O ₂ Synthesis under a Large Current Enabled by the Cathode with Highly Hydrophobic Three-Phase Architecture. ACS Catalysis, 2021, 11, 13797-13808.	5.5	59
35	Construction of a Microchannel Aeration Cathode for Producing H ₂ O ₂ via Oxygen Reduction Reaction. ACS Applied Materials & Interfaces, 2021, 13, 56045-56053.	4.0	14
36	Performance of Alternating-Current-Enhanced Anaerobic Membrane Bioreactor: Membrane Fouling, Wastewater Treatment, and CH ₄ Production. ACS Sustainable Chemistry and Engineering, 2021, 9, 15973-15982.	3.2	8

#	Article	IF	CITATIONS
37	Selective electrochemical H2O2 generation and activation on a bifunctional catalyst for heterogeneous electro-Fenton catalysis. Journal of Hazardous Materials, 2020, 382, 121102.	6.5	137
38	Efficient electrochemical reduction of nitrobenzene by nitrogen doped porous carbon. Chemosphere, 2020, 238, 124636.	4.2	25
39	Health risk assessment of heavy metals and pesticides: A case study in the main drinking water source in Dalian, China. Chemosphere, 2020, 242, 125113.	4.2	116
40	Porous carbon membrane with enhanced selectivity and antifouling capability for water treatment under electrochemical assistance. Journal of Colloid and Interface Science, 2020, 560, 59-68.	5.0	30
41	Construction of a Microchannel Electrochemical Reactor with a Monolithic Porous-Carbon Cathode for Adsorption and Degradation of Organic Pollutants in Several Minutes of Retention Time. Environmental Science & amp; Technology, 2020, 54, 1920-1928.	4.6	30
42	Tuning Lewis acidity of MIL-88B-Fe with mix-valence coordinatively unsaturated iron centers on ultrathin Ti3C2 nanosheets for efficient photo-Fenton reaction. Applied Catalysis B: Environmental, 2020, 264, 118534.	10.8	102
43	Efficient day-night photocatalysis performance of 2D/2D Ti3C2/Porous g-C3N4 nanolayers composite and its application in the degradation of organic pollutants. Chemosphere, 2020, 246, 125760.	4.2	89
44	Constructing efficient WO3-FPC system for photoelectrochemical H2O2 production and organic pollutants degradation. Chemical Engineering Journal, 2020, 389, 123427.	6.6	23
45	Conductive CNT/nanofiber composite hollow fiber membranes with electrospun support layer for water purification. Journal of Membrane Science, 2020, 596, 117613.	4.1	35
46	Single-atom platinum confined by the interlayer nanospace of carbon nitride for efficient photocatalytic hydrogen evolution. Nano Energy, 2020, 69, 104409.	8.2	185
47	Efficient and stable heterogeneous electro-Fenton system using iron oxides embedded in Cu, N co-doped hollow porous carbon as functional electrocatalyst. Separation and Purification Technology, 2020, 238, 116424.	3.9	50
48	Electrokinetic Enhancement of Water Flux and Ion Rejection through Graphene Oxide/Carbon Nanotube Membrane. Environmental Science & Technology, 2020, 54, 15433-15441.	4.6	33
49	Cross-linked Graphene Oxide Framework Membranes with Robust Nano-Channels for Enhanced Sieving Ability. Environmental Science & Technology, 2020, 54, 15442-15453.	4.6	75
50	Enhanced Photocatalytic H ₂ O ₂ Production over Carbon Nitride by Doping and Defect Engineering. ACS Catalysis, 2020, 10, 14380-14389.	5.5	265
51	High-Efficiency Electrocatalysis of Molecular Oxygen toward Hydroxyl Radicals Enabled by an Atomically Dispersed Iron Catalyst. Environmental Science & Technology, 2020, 54, 12662-12672.	4.6	114
52	Utilizing transparent and conductive SnO2 as electron mediator to enhance the photocatalytic performance of Z-scheme Si-SnO2-TiOx. Frontiers of Environmental Science and Engineering, 2020, 14, 1.	3.3	4
53	Selective electroreduction of CO2 to acetone by single copper atoms anchored on N-doped porous carbon. Nature Communications, 2020, 11, 2455.	5.8	265
54	Flexible Superhydrophobic Metal-Based Carbon Nanotube Membrane for Electrochemically Enhanced Water Treatment. Environmental Science & Technology, 2020, 54, 9074-9082.	4.6	65

#	Article	IF	CITATIONS
55	High-flux robust ceramic membranes functionally decorated with nano-catalyst for emerging micro-pollutant removal from water. Journal of Membrane Science, 2020, 611, 118281.	4.1	47
56	Opportunities for nanotechnology to enhance electrochemical treatment of pollutants in potable water and industrial wastewater – a perspective. Environmental Science: Nano, 2020, 7, 2178-2194.	2.2	74
57	Enhancing anaerobic digestion in anaerobic integrated floating fixed-film activated sludge (An-IFFAS) system using novel electron mediator suspended biofilm carriers. Water Research, 2020, 175, 115697.	5.3	36
58	Simultaneous nitriï¬cation and denitriï¬cation process using novel surface-modified suspended carriers for the treatment of real domestic wastewater. Chemosphere, 2020, 247, 125831.	4.2	97
59	Integrated Analysis of the Water–Energy–Environmental Pollutant Nexus in the Petrochemical Industry. Environmental Science & Technology, 2020, 54, 14830-14842.	4.6	17
60	Acetate production from inorganic carbon (HCO3-) in photo-assisted biocathode microbial electrosynthesis systems using WO3/MoO3/g-C3N4 heterojunctions and Serratia marcescens species. Applied Catalysis B: Environmental, 2020, 267, 118611.	10.8	69
61	Energy-transfer-mediated oxygen activation in carbonyl functionalized carbon nitride nanosheets for high-efficient photocatalytic water disinfection and organic pollutants degradation. Water Research, 2020, 177, 115798.	5.3	68
62	Mitigating Membrane Fouling Based on In Situ •OH Generation in a Novel Electro-Fenton Membrane Bioreactor. Environmental Science & Technology, 2020, 54, 7669-7676.	4.6	43
63	Intensified degradation and mineralization of antibiotic metronidazole in photo-assisted microbial fuel cells with Mo-W catalytic cathodes under anaerobic or aerobic conditions in the presence of Fe(III). Chemical Engineering Journal, 2019, 376, 119566.	6.6	37
64	Recovery of Metals from Wastes Using Bioelectrochemical Systems. , 2019, , 121-156.		1
65	Enhanced nitrification in integrated floating fixed-film activated sludge (IFFAS) system using novel clinoptilolite composite carrier. Frontiers of Environmental Science and Engineering, 2019, 13, 1.	3.3	13
66	Novel metal-organic framework supported manganese oxides for the selective catalytic reduction of NOx with NH3: Promotional role of the support. Journal of Hazardous Materials, 2019, 380, 120800.	6.5	36
67	Effects of chlorinated polyfluoroalkyl ether sulfonate in comparison with perfluoroalkyl acids on gene profiles and stemness in human mesenchymal stem cells. Chemosphere, 2019, 237, 124402.	4.2	9
68	Alkali-metal-oxides coated ultrasmall Pt sub-nanoparticles loading on intercalated carbon nitride: Enhanced charge interlayer transportation and suppressed backwark reaction for overall water splitting. Journal of Catalysis, 2019, 377, 72-80.	3.1	30
69	Nanoscale lightning rod effect in 3D carbon nitride nanoneedle: Enhanced charge collection and separation for efficient photocatalysis. Journal of Catalysis, 2019, 375, 361-370.	3.1	55
70	Vertically Aligned Janus MXene-Based Aerogels for Solar Desalination with High Efficiency and Salt Resistance. ACS Nano, 2019, 13, 13196-13207.	7.3	280
71	Efficient H2O2 generation and electro-Fenton degradation of pollutants in microchannels of oxidized monolithic-porous-carbon cathode. Water Science and Technology, 2019, 80, 970-978.	1.2	8
72	Enhanced activation of peroxymonosulfate by CNT-TiO2 under UV-light assistance for efficient degradation of organic pollutants. Frontiers of Environmental Science and Engineering, 2019, 13, 1.	3.3	28

#	Article	IF	CITATIONS
73	A pH-responsive PAA-grafted-CNT intercalated RGO membrane with steady separation efficiency for charged contaminants over a wide pH range. Separation and Purification Technology, 2019, 215, 422-429.	3.9	25
74	Carbon nanotubes-incorporated MIL-88B-Fe as highly efficient Fenton-like catalyst for degradation of organic pollutants. Frontiers of Environmental Science and Engineering, 2019, 13, 1.	3.3	49
75	Enhanced catalytic ozonation by highly dispersed CeO2 on carbon nanotubes for mineralization of organic pollutants. Journal of Hazardous Materials, 2019, 368, 621-629.	6.5	71
76	Enhanced heterogeneous activation of peroxymonosulfate by Co and N codoped porous carbon for degradation of organic pollutants: the synergism between Co and N. Environmental Science: Nano, 2019, 6, 399-410.	2.2	129
77	A novel porous-carbon-based hollow fiber membrane with electrochemical reduction mediated by in-situ hydroxyl radical generation for fouling control and water treatment. Applied Catalysis B: Environmental, 2019, 255, 117772.	10.8	46
78	Templated nanoreactor arrays for nanoscale-tunable liquid-phase catalysis. Chemical Communications, 2019, 55, 6575-6578.	2.2	3
79	Fabrication of a doubleâ€helical photocatalytic module for disinfection and antibiotics degradation. Water Environment Research, 2019, 91, 918-925.	1.3	1
80	Performing homogeneous catalytic ozonation using heterogeneous Mn ²⁺ -bonded oxidized carbon nanotubes by self-driven pH variation induced reversible desorption and adsorption of Mn ²⁺ . Environmental Science: Nano, 2019, 6, 1932-1940.	2.2	12
81	Preparation of fluorinated activated carbon for electro-Fenton treatment of organic pollutants in coking wastewater: The influences of oxygen-containing groups. Separation and Purification Technology, 2019, 224, 534-542.	3.9	33
82	Enhanced permeability, contaminants removal and antifouling ability of CNTs-based hollow fiber membranes under electrochemical assistance. Journal of Membrane Science, 2019, 582, 335-341.	4.1	28
83	Three-Dimensional Branched Crystal Carbon Nitride with Enhanced Intrinsic Peroxidase-Like Activity: A Hypersensitive Platform for Colorimetric Detection. ACS Applied Materials & Interfaces, 2019, 11, 17467-17474.	4.0	29
84	Comparison of CNT-PVA membrane and commercial polymeric membranes in treatment of emulsified oily wastewater. Frontiers of Environmental Science and Engineering, 2019, 13, 1.	3.3	23
85	Current Prospective on Environmental Nanotechnology Research in China. Environmental Science & Technology, 2019, 53, 4001-4002.	4.6	4
86	Enhanced Perfluorooctanoic Acid Degradation by Electrochemical Activation of Sulfate Solution on B/N Codoped Diamond. Environmental Science & Technology, 2019, 53, 5195-5201.	4.6	91
87	<i>In situ</i> remediation of subsurface contamination: opportunities and challenges for nanotechnology and advanced materials. Environmental Science: Nano, 2019, 6, 1283-1302.	2.2	65
88	Improvement of Antifouling and Antimicrobial Abilities on Silver–Carbon Nanotube Based Membranes under Electrochemical Assistance. Environmental Science & Technology, 2019, 53, 5292-5300.	4.6	45
89	Catalytic performance and an insight into the mechanism of CeO2 nanocrystals with different exposed facets in catalytic ozonation of p-nitrophenol. Applied Catalysis B: Environmental, 2019, 248, 526-537.	10.8	149
90	Non enzymatic fluorometric determination of glucose by using quenchable g-C3N4 quantum dots. Mikrochimica Acta, 2019, 186, 779.	2.5	10

#	Article	IF	CITATIONS
91	N-doped three-dimensional carbon foam as binder-free electrode for organic pollutants removal by electro-Fenton in neutral medium. Blue-Green Systems, 2019, 1, 86-101.	0.6	2
92	Electrochemical reduction of N ₂ to ammonia on Co single atom embedded N-doped porous carbon under ambient conditions. Journal of Materials Chemistry A, 2019, 7, 26358-26363.	5.2	51
93	Real Time Detection of Hazardous Hydroxyl Radical Using an Electrochemical Approach. ChemistrySelect, 2019, 4, 12507-12511.	0.7	14
94	Steering CO ₂ electroreduction toward ethanol production by a surface-bound Ru polypyridyl carbene catalyst on N-doped porous carbon. Proceedings of the National Academy of Sciences of the United States of America, 2019, 116, 26353-26358.	3.3	55
95	Efficient photo-Fenton activity in mesoporous MIL-100(Fe) decorated with ZnO nanosphere for pollutants degradation. Applied Catalysis B: Environmental, 2019, 245, 428-438.	10.8	187
96	A novel aerobic electrochemical membrane bioreactor with CNTs hollow fiber membrane by electrochemical oxidation to improve water quality and mitigate membrane fouling. Water Research, 2019, 151, 54-63.	5.3	73
97	The Technology Horizon for Photocatalytic Water Treatment: Sunrise or Sunset?. Environmental Science & Technology, 2019, 53, 2937-2947.	4.6	493
98	Sequential anaerobic and electro-Fenton processes mediated by W and Mo oxides for degradation/mineralization of azo dye methyl orange in photo assisted microbial fuel cells. Applied Catalysis B: Environmental, 2019, 245, 672-680.	10.8	68
99	Fabrication of g-C3N4/Ti3C2 composite and its visible-light photocatalytic capability for ciprofloxacin degradation. Separation and Purification Technology, 2019, 211, 782-789.	3.9	177
100	Constructing desired interfacial energy band alignment of Z-scheme TiO2-Pd-Cu2O hybrid by controlling the contact facet for improved photocatalytic performance. Applied Catalysis B: Environmental, 2019, 244, 347-355.	10.8	60
101	Construction of Z-Scheme g-C3N4/RGO/WO3 with in situ photoreduced graphene oxide as electron mediator for efficient photocatalytic degradation of ciprofloxacin. Chemosphere, 2019, 215, 444-453.	4.2	152
102	Improving Ion Rejection of Conductive Nanofiltration Membrane through Electrically Enhanced Surface Charge Density. Environmental Science & amp; Technology, 2019, 53, 868-877.	4.6	83
103	Novel Anaerobic Electrochemical Membrane Bioreactor with a CNTs Hollow Fiber Membrane Cathode to Mitigate Membrane Fouling and Enhance Energy Recovery. Environmental Science & amp; Technology, 2019, 53, 1014-1021.	4.6	71
104	A loop of catholyte effluent feeding to bioanodes for complete recovery of Sn, Fe, and Cu with simultaneous treatment of the co-present organics in microbial fuel cells. Science of the Total Environment, 2019, 651, 1698-1708.	3.9	25
105	Nitrogen-doped hierarchically porous carbon nanopolyhedras derived from core-shell ZIF-8@ZIF-8 single crystals for enhanced oxygen reduction reaction. Catalysis Today, 2019, 327, 366-373.	2.2	47
106	Covalent functionalization of MoS2 nanosheets synthesized by liquid phase exfoliation to construct electrochemical sensors for Cd (II) detection. Talanta, 2018, 182, 38-48.	2.9	58
107	Fouling control mechanisms in filtrating natural organic matters by electro-enhanced carbon nanotubes hollow fiber membranes. Journal of Membrane Science, 2018, 553, 54-62.	4.1	45
108	Efficient In Situ Utilization of Caustic for Sequential Recovery and Separation of Sn, Fe, and Cu in Microbial Fuel Cells. ChemElectroChem, 2018, 5, 1658-1669.	1.7	13

#	Article	IF	CITATIONS
109	Deposition and separation of W and Mo from aqueous solutions with simultaneous hydrogen production in stacked bioelectrochemical systems (BESs): Impact of heavy metals W(VI)/Mo(VI) molar ratio, initial pH and electrode material. Journal of Hazardous Materials, 2018, 353, 348-359.	6.5	9
110	Combined Effects of Surface Charge and Pore Size on Co-Enhanced Permeability and Ion Selectivity through RGO-OCNT Nanofiltration Membranes. Environmental Science & Technology, 2018, 52, 4827-4834.	4.6	79
111	Cooperative light irradiation and in-situ produced H 2 O 2 for efficient tungsten and molybdenum deposition in microbial electrolysis cells. Journal of Photochemistry and Photobiology A: Chemistry, 2018, 357, 156-167.	2.0	11
112	Anti-fouling characteristic of carbon nanotubes hollow fiber membranes by filtering natural organic pollutants. Korean Journal of Chemical Engineering, 2018, 35, 964-973.	1.2	14
113	Enhanced adsorption of ionizable antibiotics on activated carbon fiber under electrochemical assistance in continuous-flow modes. Water Research, 2018, 134, 162-169.	5.3	47
114	Constructing BiVO4-Au@CdS photocatalyst with energic charge-carrier-separation capacity derived from facet induction and Z-scheme bridge for degradation of organic pollutants. Applied Catalysis B: Environmental, 2018, 227, 258-265.	10.8	100
115	Enhanced separation performance of carbon nanotube–polyvinyl alcohol composite membranes for emulsified oily wastewater treatment under electrical assistance. Separation and Purification Technology, 2018, 197, 107-115.	3.9	50
116	Structuring phase junction between tri-s-triazine and triazine crystalline C3N4 for efficient photocatalytic hydrogen evolution. Applied Catalysis B: Environmental, 2018, 227, 153-160.	10.8	139
117	Facile Ammonia Synthesis from Electrocatalytic N ₂ Reduction under Ambient Conditions on N-Doped Porous Carbon. ACS Catalysis, 2018, 8, 1186-1191.	5.5	520
118	Highly Permeable Thin-Film Composite Forward Osmosis Membrane Based on Carbon Nanotube Hollow Fiber Scaffold with Electrically Enhanced Fouling Resistance. Environmental Science & Technology, 2018, 52, 1444-1452.	4.6	56
119	Carbon nitride with electron storage property: Enhanced exciton dissociation for high-efficient photocatalysis. Applied Catalysis B: Environmental, 2018, 236, 99-106.	10.8	99
120	Removal of binary Cr(VI) and Cd(II) from the catholyte of MFCs and determining their fate in EAB using fluorescence probes. Bioelectrochemistry, 2018, 122, 61-68.	2.4	23
121	Enhancing nitrogen removal efficiency in a dyestuff wastewater treatment plant with the IFFAS process: the pilot-scale and full-scale studies. Water Science and Technology, 2018, 77, 70-78.	1.2	7
122	Roles of magnetite and granular activated carbon in improvement of anaerobic sludge digestion. Bioresource Technology, 2018, 249, 666-672.	4.8	163
123	Amphiphilic PA-induced three-dimensional graphene macrostructure with enhanced removal of heavy metal ions. Journal of Colloid and Interface Science, 2018, 512, 853-861.	5.0	47
124	A multifunctional graphene-based nanofiltration membrane under photo-assistance for enhanced water treatment based on layer-by-layer sieving. Applied Catalysis B: Environmental, 2018, 224, 204-213.	10.8	80
125	Dependency of migration and reduction of mixed Cr2O72â [~] , Cu2+ and Cd2+ on electric field, ion exchange membrane and metal concentration in microbial fuel cells. Separation and Purification Technology, 2018, 192, 78-87.	3.9	27
126	Fluorine-doped carbon nanotubes as an efficient metal-free catalyst for destruction of organic pollutants in catalytic ozonation. Chemosphere, 2018, 190, 135-143.	4.2	75

#	Article	IF	CITATIONS
127	Imaging and distribution of Cd(II) ions in electrotrophs and its response to current and electron transfer inhibitor in microbial electrolysis cells. Sensors and Actuators B: Chemical, 2018, 255, 244-254.	4.0	20
128	Optical emission spectroscopy diagnosis of energetic Ar ions in synthesis of SiC polytypes by DC arc discharge plasma. Nano Research, 2018, 11, 1470-1481.	5.8	26
129	Enhanced H2O2 production by selective electrochemical reduction of O2 on fluorine-doped hierarchically porous carbon. Journal of Catalysis, 2018, 357, 118-126.	3.1	252
130	Effective adsorption of sulfamethoxazole, bisphenol A and methyl orange on nanoporous carbon derived from metal-organic frameworks. Journal of Environmental Sciences, 2018, 63, 250-259.	3.2	68
131	Accelerated startâ€up and microbial community structures of simultaneous nitrification and denitrification using novel suspended carriers. Journal of Chemical Technology and Biotechnology, 2018, 93, 577-584.	1.6	25
132	Direct growth of ultra-permeable molecularly thin porous graphene membranes for water treatment. Environmental Science: Nano, 2018, 5, 3004-3010.	2.2	5
133	Superpermeable nanoporous carbon-based catalytic membranes for electro-Fenton driven high-efficiency water treatment. Journal of Materials Chemistry A, 2018, 6, 23502-23512.	5.2	8
134	Two-dimensional nanomaterial based sensors for heavy metal ions. Mikrochimica Acta, 2018, 185, 478.	2.5	48
135	Transformation of Nitrogen and Iron Species during Nitrogen Removal from Wastewater via Feammox by Adding Ferrihydrite. ACS Sustainable Chemistry and Engineering, 2018, 6, 14394-14402.	3.2	54
136	Fabrication of TiOx–Si photoanode and its energetic photoelectrochemical performance. Journal of Materials Science: Materials in Electronics, 2018, 29, 12700-12706.	1.1	3
137	Enhanced photocatalytic performance of a two-dimensional BiOIO3/g-C3N4 heterostructured composite with a Z-scheme configuration. Applied Catalysis B: Environmental, 2018, 237, 947-956.	10.8	99
138	Photoelectrochemical aptasensor for sulfadimethoxine using g-C3N4 quantum dots modified with reduced graphene oxide. Mikrochimica Acta, 2018, 185, 345.	2.5	38
139	Stable Superhydrophobic Ceramic-Based Carbon Nanotube Composite Desalination Membranes. Nano Letters, 2018, 18, 5514-5521.	4.5	153
140	Improving the co-digestion performance of waste activated sludge and wheat straw through ratio optimization and ferroferric oxide supplementation. Bioresource Technology, 2018, 267, 591-598.	4.8	35
141	Comparing the mechanisms of ZVI and Fe3O4 for promoting waste-activated sludge digestion. Water Research, 2018, 144, 126-133.	5.3	179
142	Catalytic Ozonation in Arrayed Zinc Oxide Nanotubes as Highly Efficient Mini-Column Catalyst Reactors (MCRs): Augmentation of Hydroxyl Radical Exposure. Environmental Science & Technology, 2018, 52, 8701-8711.	4.6	45
143	Enhanced heterogeneous Fenton-like activity by Cu-doped BiFeO3 perovskite for degradation of organic pollutants. Frontiers of Environmental Science and Engineering, 2018, 12, 1.	3.3	26
144	Enhanced electro-Fenton performance by fluorine-doped porous carbon for removal of organic pollutants in wastewater. Chemical Engineering Journal, 2018, 354, 606-615.	6.6	91

#	Article	IF	CITATIONS
145	Two-dimensional MoS2: A promising building block for biosensors. Biosensors and Bioelectronics, 2017, 89, 56-71.	5.3	215
146	Determination of Oxytetracycline by a Graphene—Gold Nanoparticle-Based Colorimetric Aptamer Sensor. Analytical Letters, 2017, 50, 544-553.	1.0	26
147	CO ₂ Electroreduction at Low Overpotential on Oxide-Derived Cu/Carbons Fabricated from Metal Organic Framework. ACS Applied Materials & Interfaces, 2017, 9, 5302-5311.	4.0	239
148	Photochemical reactions between bromophenols and hydroxyl radical generated in aqueous solution: A laser flash photolysis study. Journal of Photochemistry and Photobiology A: Chemistry, 2017, 336, 63-68.	2.0	13
149	An Electrochemical Sensor Based on Graphene-Polypyrrole Nanocomposite for the Specific Detection of Pb (II). Nano, 2017, 12, 1750008.	0.5	22
150	Poly(vinylidene fluoride) hollowâ€fiber membranes containing silver/graphene oxide dope with excellent filtration performance. Journal of Applied Polymer Science, 2017, 134, .	1.3	21
151	High surface area mesoporous nanocast LaMO3 (M = Mn, Fe) perovskites for efficient catalytic ozonation and an insight into probable catalytic mechanism. Applied Catalysis B: Environmental, 2017, 206, 692-703.	10.8	218
152	Accelerated startup of moving bed biofilm process with novel electrophilic suspended biofilm carriers. Chemical Engineering Journal, 2017, 315, 364-372.	6.6	83
153	Enhanced activation of peroxymonosulfate by nitrogen doped porous carbon for effective removal of organic pollutants. Carbon, 2017, 115, 730-739.	5.4	372
154	Potentially direct interspecies electron transfer of methanogenesis for syntrophic metabolism under sulfate reducing conditions with stainless steel. Bioresource Technology, 2017, 234, 303-309.	4.8	86
155	Adding granular activated carbon into anaerobic sludge digestion to promote methane production and sludge decomposition. Journal of Cleaner Production, 2017, 149, 1101-1108.	4.6	247
156	Three-dimensional TiO ₂ nanotube arrays combined with g-C ₃ N ₄ quantum dots for visible light-driven photocatalytic hydrogen production. RSC Advances, 2017, 7, 13223-13227.	1.7	27
157	Towards engineering application: Potential mechanism for enhancing anaerobic digestion of complex organic waste with different types of conductive materials. Water Research, 2017, 115, 266-277.	5.3	254
158	Superpermeable Atomic-Thin Graphene Membranes with High Selectivity. ACS Nano, 2017, 11, 1920-1926.	7.3	45
159	Fluorescence microscopy image-analysis (FMI) for the characterization of interphase HOË™ production originated by heterogeneous catalysis. Chemical Communications, 2017, 53, 2575-2577.	2.2	19
160	Carbon-nanotube-based sandwich-like hollow fiber membranes for expanded microcystin-LR removal applications. Chemical Engineering Journal, 2017, 319, 212-218.	6.6	25
161	Highly sensitive detection of Cr(VI) by reduced graphene oxide chemiresistor and 1,4-dithiothreitol functionalized Au nanoparticles. Sensors and Actuators B: Chemical, 2017, 247, 265-272.	4.0	38
162	Interface evolution in the platelet-like SiC@C and SiC@SiO2 monocrystal nanocapsules. Nano Research, 2017, 10, 2644-2656.	5.8	27

#	Article	IF	CITATIONS
163	Scaling-up of a zero valent iron packed anaerobic reactor for textile dye wastewater treatment: a potential technology for on-site upgrading and rebuilding of traditional anaerobic wastewater treatment plant. Water Science and Technology, 2017, 76, 823-831.	1.2	10
164	Is A/A/O process effective in toxicity removal? Case study with coking wastewater. Ecotoxicology and Environmental Safety, 2017, 142, 363-368.	2.9	11
165	Photoinduced formation of reactive oxygen species and electrons from metal oxide–silica nanocomposite: An EPR spin-trapping study. Applied Surface Science, 2017, 416, 281-287.	3.1	36
166	Potentially shifting from interspecies hydrogen transfer to direct interspecies electron transfer for syntrophic metabolism to resist acidic impact with conductive carbon cloth. Chemical Engineering Journal, 2017, 313, 10-18.	6.6	201
167	Constructing a visible-light-driven photocatalytic membrane by g-C3N4 quantum dots and TiO2 nanotube array for enhanced water treatment. Scientific Reports, 2017, 7, 3128.	1.6	40
168	PEGylated molybdenum dichalcogenide (PEG-MoS ₂) nanosheets with enhanced peroxidase-like activity for the colorimetric detection of H ₂ O ₂ . New Journal of Chemistry, 2017, 41, 6700-6708.	1.4	42
169	Evaluation of the detoxification efficiencies of coking wastewater treated by combined anaerobic-anoxic-oxic (A 2 O) and advanced oxidation process. Journal of Hazardous Materials, 2017, 338, 186-193.	6.5	52
170	A colorimetric aptasensor for sulfadimethoxine detection based on peroxidase-like activity of graphene/nickel@palladium hybrids. Analytical Biochemistry, 2017, 525, 92-99.	1.1	46
171	Ferroelectric-enhanced Z-schematic electron transfer in BiVO 4 -BiFeO 3 -CuInS 2 for efficient photocatalytic pollutant degradation. Applied Catalysis B: Environmental, 2017, 209, 591-599.	10.8	96
172	Start-up and bacterial community compositions of partial nitrification in moving bed biofilm reactor. Applied Microbiology and Biotechnology, 2017, 101, 2563-2574.	1.7	64
173	Acute toxicity reduction and toxicity identification in pigment-contaminated wastewater during anaerobic-anoxic-oxic (A/A/O) treatment process. Chemosphere, 2017, 168, 1285-1292.	4.2	14
174	Evaluations of biofilm thickness and dissolved oxygen on single stage anammox process in an up-flow biological aerated filter. Biochemical Engineering Journal, 2017, 119, 20-26.	1.8	32
175	Cathodic Cr(VI) reduction by electrochemically active bacteria sensed by fluorescent probe. Sensors and Actuators B: Chemical, 2017, 243, 303-310.	4.0	27
176	Selective Electrochemical Reduction of Carbon Dioxide to Ethanol on a Boron―and Nitrogen oâ€doped Nanodiamond. Angewandte Chemie, 2017, 129, 15813-15817.	1.6	196
177	Selective Electrochemical Reduction of Carbon Dioxide to Ethanol on a Boron―and Nitrogen oâ€doped Nanodiamond. Angewandte Chemie - International Edition, 2017, 56, 15607-15611.	7.2	226
178	New Application of Ethanol-Type Fermentation: Stimulating Methanogenic Communities with Ethanol to Perform Direct Interspecies Electron Transfer. ACS Sustainable Chemistry and Engineering, 2017, 5, 9441-9453.	3.2	41
179	Preferable utilization of in-situ produced H2O2 rather than externally added for efficient deposition of tungsten and molybdenum in microbial fuel cells. Electrochimica Acta, 2017, 247, 880-890.	2.6	19
180	Synthesis of Z-scheme Ag2CrO4/Ag/g-C3N4 composite with enhanced visible-light photocatalytic activity for 2,4-dichlorophenol degradation. Applied Catalysis B: Environmental, 2017, 219, 439-449.	10.8	127

#	Article	IF	CITATIONS
181	Hydrothermal fabrication of few-layer MoS 2 nanosheets within nanopores on TiO 2 derived from MIL-125(Ti) for efficient photocatalytic H 2 evolution. Applied Surface Science, 2017, 426, 177-184.	3.1	53
182	Determination and prediction of octanol-air partition coefficients for organophosphate flame retardants. Ecotoxicology and Environmental Safety, 2017, 145, 283-288.	2.9	24
183	Probing the interphase "HO zone―originated by carbon nanotube during catalytic ozonation. Water Research, 2017, 122, 86-95.	5.3	72
184	Cobalt Nanoparticles Encapsulated in Porous Carbons Derived from Core–Shell ZIF67@ZIF8 as Efficient Electrocatalysts for Oxygen Evolution Reaction. ACS Applied Materials & Interfaces, 2017, 9, 28685-28694.	4.0	142
185	Innentitelbild: Selective Electrochemical Reduction of Carbon Dioxide to Ethanol on a Boron―and Nitrogen oâ€doped Nanodiamond (Angew. Chem. 49/2017). Angewandte Chemie, 2017, 129, 15678-15678.	1.6	1
186	Fe ₃ O ₄ -AuNPs anchored 2D metal–organic framework nanosheets with DNA regulated switchable peroxidase-like activity. Nanoscale, 2017, 9, 18699-18710.	2.8	122
187	Enhanced Fenton-like catalysis by iron-based metal organic frameworks for degradation of organic pollutants. Journal of Catalysis, 2017, 356, 125-132.	3.1	256
188	Efficient W and Mo deposition and separation with simultaneous hydrogen production in stacked bioelectrochemical systems. Chemical Engineering Journal, 2017, 327, 584-596.	6.6	35
189	Covering α-Fe2O3 protection layer on the surface of p-Si micropillar array for enhanced photoelectrochemical performance. Frontiers of Environmental Science and Engineering, 2017, 11, 1.	3.3	7
190	Occurrence, removal, and risk assessment of antibiotics in 12 wastewater treatment plants from Dalian, China. Environmental Science and Pollution Research, 2017, 24, 16478-16487.	2.7	96
191	Integration of membrane filtration and photoelectrocatalysis on g-C3N4/CNTs/Al2O3 membrane with visible-light response for enhanced water treatment. Journal of Membrane Science, 2017, 541, 153-161.	4.1	105
192	Fabrication of the hierarchical structure photocathode by structuring the surface nanopores on Si nanowires standing on p-Si wafer for the effective photoelectrochemical reduction of Cr(VI) in the aqueous solution. Separation and Purification Technology, 2017, 175, 454-459.	3.9	7
193	Correlation between circuital current, Cu(II) reduction and cellular electron transfer in EAB isolated from Cu(II)-reduced biocathodes of microbial fuel cells. Bioelectrochemistry, 2017, 114, 1-7.	2.4	64
194	Nitrogen-doped carbon with a high degree of graphitization derived from biomass as high-performance electrocatalyst for oxygen reduction reaction. Applied Surface Science, 2017, 396, 986-993.	3.1	71
195	Synthesis and electrochemical activities of TiC/C core-shell nanocrystals. Journal of Alloys and Compounds, 2017, 693, 500-509.	2.8	25
196	Impact of Fe(III) as an effective electron-shuttle mediator for enhanced Cr(VI) reduction in microbial fuel cells: Reduction of diffusional resistances and cathode overpotentials. Journal of Hazardous Materials, 2017, 321, 896-906.	6.5	89
197	Fluorescent probe based subcellular distribution of Cu(II) ions in living electrotrophs isolated from Cu(II)-reduced biocathodes of microbial fuel cells. Bioresource Technology, 2017, 225, 316-325.	4.8	28
198	Evaluation of sustainable acid rain control options utilizing a fuzzy TOPSIS multi-criteria decision analysis model frame work. Journal of Cleaner Production, 2017, 141, 612-625.	4.6	44

#	Article	IF	CITATIONS
199	Adsorption of Sulfamethoxazole on Nanoporous Carbon Derived from Metal-Organic Frameworks. Journal of Geoscience and Environment Protection, 2017, 05, 1-8.	0.2	5
200	Enhancement of anaerobic methanogenesis at a short hydraulic retention time via bioelectrochemical enrichment of hydrogenotrophic methanogens. Bioresource Technology, 2016, 218, 505-511.	4.8	66
201	Enhancing nitrogen removal efficiency and reducing nitrate liquor recirculation ratio by improving simultaneous nitrification and denitrification in integrated fixed-film activated sludge (IFAS) process. Water Science and Technology, 2016, 73, 827-834.	1.2	14
202	Evaluation of the detoxication efficiencies for acrylonitrile wastewater treated by a combined anaerobic oxic-aerobic biological fluidized tank (A/O-ABFT) process: Acute toxicity and zebrafish embryo toxicity. Chemosphere, 2016, 154, 1-7.	4.2	12
203	Three-Dimensional Graphene Supported Bimetallic Nanocomposites with DNA Regulated-Flexibly Switchable Peroxidase-Like Activity. ACS Applied Materials & Interfaces, 2016, 8, 9855-9864.	4.0	89
204	A controlled wet-spinning and dip-coating process for preparation of high-permeable TiO2 hollow fiber membranes. Water Science and Technology, 2016, 73, 725-733.	1.2	2
205	Unique three dimensional architecture using a metal-free semiconductor cross-linked bismuth vanadate for efficient photoelectrochemical water oxidation. Nano Energy, 2016, 24, 148-157.	8.2	44
206	High desalination permeability, wetting and fouling resistance on superhydrophobic carbon nanotube hollow fiber membrane under self-powered electrochemical assistance. Journal of Membrane Science, 2016, 514, 501-509.	4.1	64
207	Fabrication of TiO2 nanofiber membranes by a simple dip-coating technique for water treatment. Surface and Coatings Technology, 2016, 298, 45-52.	2.2	43
208	Novel <i>in situ</i> Synthesized Fe@C Magnetic Nanocapsules Used as Adsorbent for Removal of Organic Dyes and its Recycling. Nano, 2016, 11, 1650013.	0.5	7
209	Nitrogen and sulfur co-doped graphene/carbon nanotube as metal-free electrocatalyst for oxygen evolution reaction: the enhanced performance by sulfur doping. Electrochimica Acta, 2016, 204, 169-175.	2.6	93
210	Fabrication of Au/CNT hollow fiber membrane for 4-nitrophenol reduction. RSC Advances, 2016, 6, 41114-41121.	1.7	33
211	Ceramic membrane separation coupled with catalytic ozonation for tertiary treatment of dyestuff wastewater in a pilot-scale study. Chemical Engineering Journal, 2016, 301, 19-26.	6.6	67
212	A versatile fluorescent biosensor based on target-responsive graphene oxide hydrogel for antibiotic detection. Biosensors and Bioelectronics, 2016, 83, 267-273.	5.3	123
213	An electrochemical sensor based on molecularly imprinted polypyrrole/graphene quantum dots composite for detection of bisphenol A in water samples. Sensors and Actuators B: Chemical, 2016, 233, 599-606.	4.0	187
214	Integration of microfiltration and visible-light-driven photocatalysis on g-C 3 N 4 nanosheet/reduced graphene oxide membrane for enhanced water treatment. Applied Catalysis B: Environmental, 2016, 194, 134-140.	10.8	189
215	Joint toxicity of cadmium and SDBS on Daphnia magna and Danio rerio. Ecotoxicology, 2016, 25, 1703-1711.	1.1	13
216	Synthesis of manganese incorporated hierarchical mesoporous silica nanosphere with fibrous morphology by facile one-pot approach for efficient catalytic ozonation. Journal of Hazardous Materials, 2016, 318, 308-318.	6.5	44

#	Article	IF	CITATIONS
217	Enhanced Cd(II) removal with simultaneous hydrogen production in biocathode microbial electrolysis cells in the presence of acetate or NaHCO 3. International Journal of Hydrogen Energy, 2016, 41, 13368-13379.	3.8	63
218	Communities stimulated with ethanol to perform direct interspecies electron transfer for syntrophic metabolism of propionate and butyrate. Water Research, 2016, 102, 475-484.	5.3	241
219	Electrochemical reduction of carbon dioxide to formate with Fe-C electrodes in anaerobic sludge digestion process. Water Research, 2016, 106, 339-343.	5.3	37
220	Nutrient removal performance and microbial characteristics of a full-scale IFAS-EBPR process treating municipal wastewater. Water Science and Technology, 2016, 73, 1261-1268.	1.2	26
221	Network optimization and performance evaluation of the water-use system in China's straw pulp and paper industry: a case study. Clean Technologies and Environmental Policy, 2016, 18, 257-268.	2.1	9
222	Dynamic adsorption of ciprofloxacin on carbon nanofibers: Quantitative measurement by in situ fluorescence. Journal of Water Process Engineering, 2016, 9, e14-e20.	2.6	61
223	Cooperative cathode electrode and in situ deposited copper for subsequent enhanced Cd(II) removal and hydrogen evolution in bioelectrochemical systems. Bioresource Technology, 2016, 200, 565-571.	4.8	58
224	Enhancement of sludge granulation in hydrolytic acidogenesis by denitrification. Applied Microbiology and Biotechnology, 2016, 100, 3313-3320.	1.7	14
225	A visible and label-free colorimetric sensor for miRNA-21 detection based on peroxidase-like activity of graphene/gold-nanoparticle hybrids. Analytical Methods, 2016, 8, 2005-2012.	1.3	57
226	Producing nitrite from anodic ammonia oxidation to accelerate anammox in a bioelectrochemical system with a given anode potential. Chemical Engineering Journal, 2016, 291, 184-191.	6.6	36
227	Electricity generation and bivalent copper reduction as a function of operation time and cathode electrode material in microbial fuel cells. Journal of Power Sources, 2016, 307, 705-714.	4.0	68
228	Electrolytic exfoliation synthesis of boron doped graphene quantum dots: a new luminescent material for electrochemiluminescence detection of oncogene microRNA-20a. Electrochimica Acta, 2016, 190, 1150-1158.	2.6	70
229	Enriching functional microbes with electrode to accelerate the decomposition of complex substrates during anaerobic digestion of municipal sludge. Biochemical Engineering Journal, 2016, 111, 1-9.	1.8	30
230	Enhanced decomposition of waste activated sludge via anodic oxidation for methane production and bioenergy recovery. International Biodeterioration and Biodegradation, 2016, 106, 161-169.	1.9	70
231	An Electrochemical Sensor based on p-aminothiophenol/Au Nanoparticle-Decorated H TiS2 Nanosheets for Specific Detection of Picomolar Cu (II). Electrochimica Acta, 2016, 190, 480-489.	2.6	18
232	Uncovering the Key Role of the Fermi Level of the Electron Mediator in a Z-Scheme Photocatalyst by Detecting the Charge Transfer Process of WO ₃ -metal-gC ₃ N ₄ (Metal = Cu, Ag, Au). ACS Applied Materials & Interfaces, 2016, 8, 2111-2119.	4.0	334
233	Nanocarbon-based membrane filtration integrated with electric field driving for effective membrane fouling mitigation. Water Research, 2016, 88, 285-292.	5.3	89
234	Effect of temperature on functional bacterial abundance and community structure in CANON process. Biochemical Engineering Journal, 2016, 105, 306-313.	1.8	22

#	Article	IF	CITATIONS
235	Evaluation on direct interspecies electron transfer in anaerobic sludge digestion of microbial electrolysis cell. Bioresource Technology, 2016, 200, 235-244.	4.8	157
236	Fabrication of pilot-scale photocatalytic disinfection device by installing TiO2 coated helical support into UV annular reactor for strengthening sterilization. Chemical Engineering Journal, 2016, 283, 1506-1513.	6.6	40
237	Enhanced catalytic activity over MIL-100(Fe) loaded ceria catalysts for the selective catalytic reduction of NO x with NH 3 at low temperature. Journal of Hazardous Materials, 2016, 301, 512-521.	6.5	68
238	Enhancing nitrogen and phosphorus removal in the BUCT–IFAS process by bypass flow strategy. Water Science and Technology, 2015, 72, 528-534.	1.2	6
239	Three-Dimensional Porous H _{<i>x</i>} TiS ₂ Nanosheet–Polyaniline Nanocomposite Electrodes for Directly Detecting Trace Cu(II) Ions. Analytical Chemistry, 2015, 87, 5605-5613.	3.2	39
240	Integration of membrane filtration and photoelectrocatalysis using a TiO2/carbon/Al2O3 membrane for enhanced water treatment. Journal of Hazardous Materials, 2015, 299, 27-34.	6.5	50
241	Monohydroxylated Polybrominated Diphenyl Ethers (OH-PBDEs) and Dihydroxylated Polybrominated Biphenyls (Di-OH-PBBs): Novel Photoproducts of 2,6-Dibromophenol. Environmental Science & Technology, 2015, 49, 14120-14128.	4.6	20
242	Fluorescent biosensor for sensitive analysis of oxytetracycline based on an indirectly labelled long-chain aptamer. RSC Advances, 2015, 5, 58895-58901.	1.7	32
243	Formation mechanism and optical characterization of polymorphic silicon nanostructures by DC arc-discharge. RSC Advances, 2015, 5, 68714-68721.	1.7	28
244	Visible assay for glycosylase based on intrinsic catalytic ability of graphene/gold nanoparticles hybrids. Biosensors and Bioelectronics, 2015, 68, 7-13.	5.3	37
245	Effects of an electric field and iron electrode on anaerobic denitrification at low C/N ratios. Chemical Engineering Journal, 2015, 266, 241-248.	6.6	43
246	Effects of developmental perfluorooctane sulfonate exposure on spatial learning and memory ability of rats and mechanism associated with synaptic plasticity. Food and Chemical Toxicology, 2015, 76, 70-76.	1.8	54
247	Enhancement of sludge granulation in anaerobic acetogenesis by addition of nitrate and microbial community analysis. Biochemical Engineering Journal, 2015, 95, 104-111.	1.8	13
248	Comparison of Co(II) reduction on three different cathodes of microbial electrolysis cells driven by Cu(II)-reduced microbial fuel cells under various cathode volume conditions. Chemical Engineering Journal, 2015, 266, 121-132.	6.6	32
249	A pilot-scale coupling catalytic ozonation–membrane filtration system for recirculating aquaculture wastewater treatment. Desalination, 2015, 363, 37-43.	4.0	50
250	Enhanced Permeability, Selectivity, and Antifouling Ability of CNTs/Al ₂ O ₃ Membrane under Electrochemical Assistance. Environmental Science & Technology, 2015, 49, 2293-2300.	4.6	128
251	An electrochemiluminescence sensing for DNA glycosylase assay with enhanced host-guest recognition technique based on α-cyclodextrin functionalized gold/silica cell-shell nanoparticles. Electrochimica Acta, 2015, 157, 54-61.	2.6	10
252	Electrochemical DNA sensor for specific detection of picomolar Hg(<scp>ii</scp>) based on exonuclease III-assisted recycling signal amplification. Analyst, The, 2015, 140, 2029-2036.	1.7	25

#	Article	IF	CITATIONS
253	An electrochemical sensor for selective determination of sulfamethoxazole in surface water using a molecularly imprinted polymer modified BDD electrode. Analytical Methods, 2015, 7, 2693-2698.	1.3	50
254	The role of lattice oxygen on the activity and selectivity of the OMS-2 catalyst for the total oxidation of toluene. Chemical Engineering Journal, 2015, 270, 58-65.	6.6	353
255	Zero-valent iron enhanced methanogenic activity in anaerobic digestion of waste activated sludge after heat and alkali pretreatment. Waste Management, 2015, 38, 297-302.	3.7	73
256	Adsorption of ciprofloxacin, bisphenol and 2-chlorophenol on electrospun carbon nanofibers: In comparison with powder activated carbon. Journal of Colloid and Interface Science, 2015, 447, 120-127.	5.0	142
257	Using three-bio-electrode reactor to enhance the activity of anammox biomass. Bioresource Technology, 2015, 196, 376-382.	4.8	46
258	Photochemical Formation of Hydroxylated Polybrominated Diphenyl Ethers (OH-PBDEs) from Polybrominated Diphenyl Ethers (PBDEs) in Aqueous Solution under Simulated Solar Light Irradiation. Environmental Science & Technology, 2015, 49, 9092-9099.	4.6	35
259	Perfluorooctane sulfonate induces apoptosis of hippocampal neurons in rat offspring associated with calcium overload. Toxicology Research, 2015, 4, 931-938.	0.9	12
260	Potential for direct interspecies electron transfer in an electric-anaerobic system to increase methane production from sludge digestion. Scientific Reports, 2015, 5, 11094.	1.6	138
261	Voltage-Gated Transport of Nanoparticles across Free-Standing All-Carbon-Nanotube-Based Hollow-Fiber Membranes. ACS Applied Materials & Interfaces, 2015, 7, 14620-14627.	4.0	14
262	Adaptively Evolving Bacterial Communities for Complete and Selective Reduction of Cr(VI), Cu(II), and Cd(II) in Biocathode Bioelectrochemical Systems. Environmental Science & Technology, 2015, 49, 9914-9924.	4.6	140
263	Carbon nanotube hollow fiber membranes: High-throughput fabrication, structural control and electrochemically improved selectivity. Journal of Membrane Science, 2015, 493, 97-105.	4.1	38
264	Fabrication of quantum-sized CdS-coated TiO2 nanotube array with efficient photoelectrochemical performance using modified successive ionic layer absorption and reaction (SILAR) method. Science Bulletin, 2015, 60, 1281-1286.	4.3	30
265	Complete separation of Cu(II), Co(II) and Li(I) using self-driven MFCs–MECs with stainless steel mesh cathodes under continuous flow conditions. Separation and Purification Technology, 2015, 147, 114-124.	3.9	23
266	FeO enhanced acetification of propionate and granulation of sludge in acidogenic reactor. Applied Microbiology and Biotechnology, 2015, 99, 6083-6089.	1.7	14
267	High‥ield Electrosynthesis of Hydrogen Peroxide from Oxygen Reduction by Hierarchically Porous Carbon. Angewandte Chemie - International Edition, 2015, 54, 6837-6841.	7.2	419
268	Improved Photocatalytic Performance of Heterojunction by Controlling the Contact Facet: High Electron Transfer Capacity between TiO ₂ and the {110} Facet of BiVO ₄ Caused by Suitable Energy Band Alignment. Advanced Functional Materials, 2015, 25, 3074-3080.	7.8	164
269	Constructing metal-free polyimide/g-C ₃ N ₄ with high photocatalytic activity under visible light irradiation. RSC Advances, 2015, 5, 83225-83231.	1.7	28
270	Efficient Mineralization of Perfluorooctanoate by Electro-Fenton with H ₂ O ₂ Electro-generated on Hierarchically Porous Carbon. Environmental Science & Technology, 2015, 49, 13528-13533.	4.6	174

XIE QUAN

Article	IF	CITATIONS
Efficient Electrochemical Reduction of Carbon Dioxide to Acetate on Nitrogen-Doped Nanodiamond. Journal of the American Chemical Society, 2015, 137, 11631-11636.	6.6	458
Novel phosphorus doped carbon nitride modified TiO ₂ nanotube arrays with improved photoelectrochemical performance. Nanoscale, 2015, 7, 16282-16289.	2.8	96
Enhancement of anaerobic acidogenesis by integrating an electrochemical system into an acidogenic reactor: Effect of hydraulic retention times (HRT) and role of bacteria and acidophilic methanogenic Archaea. Bioresource Technology, 2015, 179, 43-49.	4.8	40
Enhanced production of methane from waste activated sludge by the combination of high-solid anaerobic digestion and microbial electrolysis cell with iron–graphite electrode. Chemical Engineering Journal, 2015, 259, 787-794.	6.6	191
Bio-electrochemical enhancement of anaerobic reduction of nitrobenzene and its effects on microbial community. Biochemical Engineering Journal, 2015, 94, 85-91.	1.8	34
Assessment of five different cathode materials for Co(II) reduction with simultaneous hydrogen evolution in microbial electrolysis cells. International Journal of Hydrogen Energy, 2015, 40, 184-196.	3.8	46
Impact of dissolved organic matter on the photolysis of the ionizable antibiotic norfloxacin. Journal of Environmental Sciences, 2015, 27, 115-123.	3.2	50
A new clean approach for production of cobalt dihydroxide from aqueous Co(II) using oxygen-reducing biocathode microbial fuel cells. Journal of Cleaner Production, 2015, 86, 441-446.	4.6	61
Anaerobic biodecolorization of AO7 by a newly isolated Fe(III)-reducing bacterium <i>Sphingomonas</i> strain DJ. Journal of Chemical Technology and Biotechnology, 2015, 90, 158-165.	1.6	18
Biological uptake and depuration of sulfadiazine and sulfamethoxazole in common carp (Cyprinus) Tj ETQq0 0 0	rgBT/Over 4.2	rlock 10 Tf 50 47
Electrochemiluminescence immunosensor for highly sensitive detection of 8-hydroxy-2′-deoxyguanosine based on carbon quantum dot coated Au/SiO2 core–shell nanoparticles. Talanta, 2015, 131, 379-385.	2.9	44
Dependency of simultaneous Cr(VI), Cu(II) and Cd(II) reduction on the cathodes of microbial electrolysis cells self-driven by microbial fuel cells. Journal of Power Sources, 2015, 273, 1103-1113.	4.0	82
Catalytic ozonation of reactive red X-3B in aqueous solution under low pressure: decolorization and OH· generation. Frontiers of Environmental Science and Engineering, 2015, 9, 591-595.	3.3	3
Clickable SBAâ€15 to Screen Functional Groups for Adsorption of Antibiotics. Chemistry - an Asian Journal, 2014, 9, 908-914.	1.7	12
Effective adsorption of 2,4-dichlorophenol on hydrogenated graphene: kinetics and isotherms. Science Bulletin, 2014, 59, 4752-4757.	1.7	2
Origin of Visible Light Photocatalytic Activity of Ag _{3} AsO _{4} from First-Principles Calculation. International Journal of Photoenergy, 2014, 2014, 1-5.	1.4	10
Preparation and characterization of vertically columnar boron doped diamond array electrode. Applied Surface Science, 2014, 303, 419-424.	3.1	17
	Efficient Electrochemical Reduction of Carbon Dioxide to Acetate on Nitrogen-Doped Nanodiamond. Journal of the American Chemical Society, 2015, 137, 11631-11636. Novel phosphorus doped carbon nitride modified TiO: sub 52 (sub> nanotube arrays with improved photoelectrochemical performance. Nanoscale, 2015, 7, 16282-16289. Enhancement of anaerobic acidogenesis by integrating an electrochemical system into an acidogenic reactor: Effect of hydraulic retention times (HRT) and role of bacteria and acidophilic methanogenic Archaea. Biorsource Technology, 2015, 179, 43-49. Enhanced production of methane from waste activated sludge by the combination of high-solid anaerobic digestion and microbial electrolysis cell with iron&E [*] graphite electrode. Chemical Engineering Journal, 2015, 299, 787-794. Bio-electrochemical enhancement of anserobic reduction of nitrobenzene and its effects on microbial community. Biochemical Engineering Journal, 2015, 94, 85-91. Assessment of five different cathode materials for Co(II) reduction with simultaneous hydrogen evolution in microbial electrolysis cells. International Journal of Hydrogen Energy, 2015, 40, 184-196. Impact of dissolved organic matter on the photolysis of the ionizable antibiotic norfloxacin. Journal of Environmental Sciences, 2015, 27, 115-123. A new clean approach for production of cobalt dihydroxide from aqueous Co(II) using oxygen/reducing biocathode microbial fuel cells. Journal of Chemical Technology and Biotechnology, 2015, 90, 158-165. Biological uptake and depuration of sulfadiazine and sulfamethoxazole in common carp (Cyprinus) Tj ETQQ00 0 electrolysis cells self-driven by microbial fuel cells. Journal of Chewer Sources, 2015, 273, 1103-1113.	Efficient Electrochemical Reduction of Carbon Dioxids to Acatate on Nitrogen-Doped Nanodiamond. 6.0 Journal of the American Chemical Society, 2015, 137, 11631-11636. 6.0 Novel phosphorus doped carbon nitride modified TiO sub32 (slubs nanotube arrays with improved photoelectrochemical performance. Nanoscale, 2015, 7, 16282-16289. 2.8 Enhancement of americable addogeness by integrating an electrochemical system into an acidogenic reactor: Effect of hydraulic returbion times (HTP) and role of bacteria ad acidophille methanogenic Acchesa. Bioresource Lechnology, 2015, 179, 43-49. 4.8 Enhanced production of methane from waste activated sludge by the combination of high-solid anaerobic digestion and microbial electrolysis cell with iron82° graphite electrode. Chemical Engineering Journal, 2015, 293, 787-794. 1.8 Bio-electrochemical enhancement of anaerobic reduction of httrobergene and its effects on interobial community. Biochemical Engineering Journal, 2015, 94, 459-1. 1.8 Assessment of five different cathode materials for Co(II) reduction with simultaneous hydrogen evolution in microbial electrolysis cells. International Journal of Hydrogen Energy, 2015, 40, 184-196. 9.8 Impact of dissolved organic matter on the photolysis of the ionizable antibiotic norfloxacin. Journal of Environmental Sciences, 2015, 27, 115-123. 4.0 Anaerobic biodecolorization of AO7 by a newly toolated Fe(III) reducing exterioric Sphingmononas (Io stran D). Journal of Chemical Technology and Biotechnology, 2015, 90, 158-165. 1.0 Biological uptake and depuration of sulfadazine and

288Molecularly imprinted polymer/mesoporous carbon nanoparticles as electrode sensing material for
selective detection of ofloxacin. Materials Letters, 2014, 129, 95-97.1.335

XIE QUAN

#	Article	IF	CITATIONS
289	Enhanced high-solids anaerobic digestion of waste activated sludge by the addition of scrap iron. Bioresource Technology, 2014, 159, 297-304.	4.8	138
290	Reduction of acute toxicity and genotoxicity of dye effluent using Fenton-coagulation process. Journal of Hazardous Materials, 2014, 274, 198-204.	6.5	54
291	Electrocatalytic debromination of BDE-47 at palladized graphene electrode. Frontiers of Environmental Science and Engineering, 2014, 8, 180-187.	3.3	2
292	Bioaccumulation and elimination kinetics of hydroxylated polybrominated diphenyl ethers (2′-OH-BDE68 and 4-OH-BDE90) and their distribution pattern in common carp (Cyprinus carpio). Journal of Hazardous Materials, 2014, 274, 16-23.	6.5	16
293	Clickable Periodic Mesoporous Organosilicas: Synthesis, Click Reactions, and Adsorption of Antibiotics. Chemistry - A European Journal, 2014, 20, 1957-1963.	1.7	50
294	Complete cobalt recovery from lithium cobalt oxide in self-driven microbial fuel cell – Microbial electrolysis cell systems. Journal of Power Sources, 2014, 259, 54-64.	4.0	73
295	Fabrication of graphene wrapped ZnIn2S4microspheres heterojunction with enhanced interfacial contact and its improved photocatalytic performance. Dalton Transactions, 2014, 43, 2888-2894.	1.6	46
296	Atomic single layer graphitic-C ₃ N ₄ : fabrication and its high photocatalytic performance under visible light irradiation. RSC Advances, 2014, 4, 624-628.	1.7	152
297	Ultrasensitive immunoassay of microcystins-LR using G-quadruplex DNAzyme as an electrocatalyst. International Journal of Environmental Analytical Chemistry, 2014, 94, 988-1000.	1.8	9
298	Porous metal–organic framework MIL-100(Fe) as an efficient catalyst for the selective catalytic reduction of NO _x with NH ₃ . RSC Advances, 2014, 4, 48912-48919.	1.7	80
299	A ZIF-8-based platform for the rapid and highly sensitive detection of indoor formaldehyde. RSC Advances, 2014, 4, 36444-36450.	1.7	26
300	Electrochemically enhanced adsorption of PFOA and PFOS on multiwalled carbon nanotubes in continuous flow mode. Science Bulletin, 2014, 59, 2890-2897.	1.7	17
301	Constructing All Carbon Nanotube Hollow Fiber Membranes with Improved Performance in Separation and Antifouling for Water Treatment. Environmental Science & Technology, 2014, 48, 8062-8068.	4.6	53
302	Photocatalytic Oxidation of Aqueous Ammonia Using Atomic Single Layer Graphitic-C ₃ N ₄ . Environmental Science & Technology, 2014, 48, 11984-11990.	4.6	204
303	Photochemical transformation of 2,2′,4,4′-tetrabromodiphenyl ether (BDE-47) in surface coastal waters: Effects of chloride and ferric ions. Marine Pollution Bulletin, 2014, 86, 76-83.	2.3	23
304	Efficient H2 production over Au/graphene/TiO2 induced by surface plasmon resonance of Au and band-gap excitation of TiO2. Materials Research Bulletin, 2014, 59, 111-116.	2.7	12
305	Enhanced anaerobic fermentation with azo dye as electron acceptor: Simultaneous acceleration of organics decomposition and azo decolorization. Journal of Environmental Sciences, 2014, 26, 1970-1976.	3.2	16
306	Ultra-thin g-C3N4 nanosheets wrapped silicon nanowire array for improved chemical stability and enhanced photoresponse. Materials Research Bulletin, 2014, 59, 179-184.	2.7	12

#	Article	IF	CITATIONS
307	Fabrication of graphene quantum dots/silicon nanowires nanohybrids for photoelectrochemical detection of microcystin-LR. Sensors and Actuators B: Chemical, 2014, 196, 532-538.	4.0	49
308	A direct approach for enhancing the performance of a microbial electrolysis cell (MEC) combined anaerobic reactor by dosing ferric iron: Enrichment and isolation of Fe(III) reducing bacteria. Chemical Engineering Journal, 2014, 248, 223-229.	6.6	18
309	Nitrogen-doped diamond electrode shows high performance for electrochemical reduction of nitrobenzene. Journal of Hazardous Materials, 2014, 265, 185-190.	6.5	41
310	Nitrogen-doped nanodiamond rod array electrode with superior performance for electroreductive debromination of polybrominated diphenyl ethers. Applied Catalysis B: Environmental, 2014, 154-155, 206-212.	10.8	30
311	Selective catalytic reaction of NOx with NH3 over Ce–Fe/TiO2-loaded wire-mesh honeycomb: Resistance to SO2 poisoning. Applied Catalysis B: Environmental, 2014, 150-151, 630-635.	10.8	116
312	Fabrication of atomic single layer graphitic-C3N4 and its high performance of photocatalytic disinfection under visible light irradiation. Applied Catalysis B: Environmental, 2014, 152-153, 46-50.	10.8	394
313	Electrochemically enhanced adsorption of nonylphenol on carbon nanotubes: Kinetics and isotherms study. Journal of Colloid and Interface Science, 2014, 415, 159-164.	5.0	26
314	Cobalt recovery with simultaneous methane and acetate production in biocathode microbial electrolysis cells. Chemical Engineering Journal, 2014, 253, 281-290.	6.6	79
315	Photoelectrocatalytic oxidation of aqueous ammonia using TiO2 nanotube arrays. Applied Surface Science, 2014, 311, 851-857.	3.1	45
316	Photodegradation of 2,4-D induced by NO2â^' in aqueous solutions: The role of NO2. Journal of Environmental Sciences, 2014, 26, 1383-1387.	3.2	5
317	Enhanced anaerobic digestion of waste activated sludge digestion by the addition of zero valent iron. Water Research, 2014, 52, 242-250.	5.3	494
318	Efficient and durable hydrogen evolution electrocatalyst based on nonmetallic nitrogen doped hexagonal carbon. Scientific Reports, 2014, 4, 6843.	1.6	78
319	Bioelectrochemical enhancement of anaerobic methanogenesis for high organic load rate wastewater treatment in a up-flow anaerobic sludge blanket (UASB) reactor. Scientific Reports, 2014, 4, 6658.	1.6	68
320	Enhanced anaerobic digestion of organic contaminants containing diverse microbial population by combined microbial electrolysis cell (MEC) and anaerobic reactor under Fe(III) reducing conditions. Bioresource Technology, 2013, 136, 273-280.	4.8	56
321	Preparation of molecularly imprinted polymer nanoparticles for selective removal of fluoroquinolone antibiotics in aqueous solution. Journal of Hazardous Materials, 2013, 244-245, 750-757.	6.5	102
322	Low-temperature selective catalytic reduction of NOx with NH3 over hierarchically macro-mesoporous Mn/TiO2. Catalysis Communications, 2013, 42, 10-13.	1.6	53
323	Multi-walled carbon nanotubes immobilized on zero-valent iron plates (Fe0-CNTs) for catalytic ozonation of methylene blue as model compound in a bubbling reactor. Separation and Purification Technology, 2013, 116, 351-359.	3.9	41
324	Intensified internal electrolysis for degradation of methylene blue as model compound induced by a novel hybrid material: Multi-walled carbon nanotubes immobilized on zero-valent iron plates (FeO-CNTs). Chemical Engineering Journal, 2013, 217, 99-107.	6.6	48

#	Article	IF	CITATIONS
325	Cobalt leaching from lithium cobalt oxide in microbial electrolysis cells. Chemical Engineering Journal, 2013, 220, 72-80.	6.6	19
326	Fluorescent assay for oxytetracycline based on a long-chain aptamer assembled onto reduced graphene oxide. Mikrochimica Acta, 2013, 180, 829-835.	2.5	57
327	Hierarchically porous silicon with significantly improved photocatalytic oxidation capability for phenol degradation. Applied Catalysis B: Environmental, 2013, 138-139, 427-433.	10.8	30
328	Evaluation of removal efficiency for acute toxicity and genotoxicity on zebrafish in anoxic–oxic process from selected municipal wastewater treatment plants. Chemosphere, 2013, 90, 2662-2666.	4.2	28
329	Selective catalytic oxidation of ammonia to nitrogen over CuO-CeO2 mixed oxides prepared by surfactant-templated method. Applied Catalysis B: Environmental, 2013, 134-135, 153-166.	10.8	149
330	Growth of tungsten oxide on carbon nanowalls templates. Materials Research Bulletin, 2013, 48, 1304-1307.	2.7	10
331	Biological sulfate reduction in the acidogenic phase of anaerobic digestion under dissimilatory Fe (III) – Reducing conditions. Water Research, 2013, 47, 2033-2040.	5.3	48
332	CNTs–TiO2/Al2O3 composite membrane with a photocatalytic function: Fabrication and energetic performance in water treatment. Separation and Purification Technology, 2013, 116, 360-365.	3.9	39
333	Uptake of perfluorooctane sulfonate (PFOS) by wheat (Triticum aestivum L.) plant. Chemosphere, 2013, 91, 139-144.	4.2	58
334	Selective catalytic oxidation of ammonia to N2 over wire–mesh honeycomb catalyst in simulated synthetic ammonia stream. Chemical Engineering Journal, 2013, 233, 233-241.	6.6	19
335	Effects of ferric iron on the anaerobic treatment and microbial biodiversity in a coupled microbial electrolysis cell (MEC) – Anaerobic reactor. Water Research, 2013, 47, 5719-5728.	5.3	104
336	A graphene and multienzyme functionalized carbon nanosphere-based electrochemical immunosensor for microcystin-LR detection. Colloids and Surfaces B: Biointerfaces, 2013, 103, 38-44.	2.5	44
337	Adding Fe0 powder to enhance the anaerobic conversion of propionate to acetate. Biochemical Engineering Journal, 2013, 73, 80-85.	1.8	133
338	Cobalt implanted TiO ₂ nanocatalyst for heterogeneous activation of peroxymonosulfate. RSC Advances, 2013, 3, 520-525.	1.7	77
339	Synergetic interactions improve cobalt leaching from lithium cobalt oxide in microbial fuel cells. Bioresource Technology, 2013, 128, 539-546.	4.8	72
340	Hierarchical porous ceramic membrane with energetic ozonation capability for enhancing water treatment. Journal of Membrane Science, 2013, 431, 197-204.	4.1	40
341	Porous LiMn2O4 microspheres as durable high power cathode materials for lithium ion batteries. Journal of Materials Chemistry A, 2013, 1, 8170.	5.2	65
342	Bioanodes/biocathodes formed at optimal potentials enhance subsequent pentachlorophenol degradation and power generation from microbial fuel cells. Bioelectrochemistry, 2013, 94, 13-22.	2.4	54

#	Article	IF	CITATIONS
343	Boron and Nitrogen Codoped Nanodiamond as an Efficient Metal-Free Catalyst for Oxygen Reduction Reaction. Journal of Physical Chemistry C, 2013, 117, 14992-14998.	1.5	80
344	Tuning the electrochemical properties of a boron and nitrogen codoped nanodiamond rod array to achieve high performance for both electro-oxidation and electro-reduction. Journal of Materials Chemistry A, 2013, 1, 14706.	5.2	16
345	A universal immunosensing strategy based on regulation of the interaction between graphene and graphene quantum dots. Chemical Communications, 2013, 49, 234-236.	2.2	156
346	The Formation Mechanism of Ag/SBA-15 Nanocomposites Prepared via <i>In-Situ</i> pH-Adjusting Method. Journal of Nanoscience and Nanotechnology, 2013, 13, 4573-4580.	0.9	8
347	Green Synthesis of Feather-Shaped MoS ₂ /CdS Photocatalyst for Effective Hydrogen Production. International Journal of Photoenergy, 2013, 2013, 1-5.	1.4	8
348	Colorimetric Detection of Melamine Based on Poly-Thymine Stabilized Gold Nanoparticles. Advanced Materials Research, 2013, 790, 619-622.	0.3	0
349	Electrochemical Sensor Based on Molecularly Imprinted Carbon Nanotubes for Selective Determination of Bisphenol A. Applied Mechanics and Materials, 2013, 303-306, 170-179.	0.2	0
350	Surfaceâ€Passivated SBAâ€15â€Supported Gold Nanoparticles: Highly Improved Catalytic Activity and Selectivity toward Hydrophobic Substrates. Chemistry - an Asian Journal, 2013, 8, 934-938.	1.7	17
351	Fabrication and Visible Response of Au-TiO ₂ (P25) Composite Photocatalyst with Obvious Surface Plasmon Resonance Effect. Advanced Materials Research, 2012, 465, 215-219.	0.3	0
352	Selectively Electrochemical Determination of Chloramphenicol in Aqueous Solution Using Molecularly Imprinted Polymer-Carbon Nanotubes-Gold Nanoparticles Modified Electrode. Journal of the Electrochemical Society, 2012, 159, J231-J236.	1.3	29
353	Colloidal Graphene as a Transducer in Homogeneous Fluorescence-Based Immunosensor for Rapid and Sensitive Analysis of Microcystin-LR. Environmental Science & Technology, 2012, 46, 12567-12574.	4.6	60
354	Enhanced azo dye wastewater treatment in a two-stage anaerobic system with FeO dosing. Bioresource Technology, 2012, 121, 148-153.	4.8	43
355	Enhancement of Catalytic Activity Over the Iron-Modified Ce/TiO ₂ Catalyst for Selective Catalytic Reduction of NO _{<i>x</i>} with Ammonia. Journal of Physical Chemistry C, 2012, 116, 25319-25327.	1.5	189
356	Improvement of Water-, Sulfur Dioxide-, and Dust-Resistance in Selective Catalytic Reduction of NO _{<i>x</i>} with NH ₃ Using a Wire-Mesh Honeycomb Catalyst. Industrial & Engineering Chemistry Research, 2012, 51, 7867-7873.	1.8	14
357	Global Liver Proteome Analysis Using iTRAQ Labeling Quantitative Proteomic Technology to Reveal Biomarkers in Mice Exposed to Perfluorooctane Sulfonate (PFOS). Environmental Science & Technology, 2012, 46, 12170-12177.	4.6	51
358	Electricity assisted anaerobic treatment of salinity wastewater and its effects on microbial communities. Water Research, 2012, 46, 3535-3543.	5.3	87
359	Detection of influenza A virus based on fluorescence resonance energy transfer from quantum dots to carbon nanotubes. Analytica Chimica Acta, 2012, 723, 83-87.	2.6	54
360	An electrochemically enhanced solid-phase microextraction approach based on molecularly imprinted polypyrrole/multi-walled carbon nanotubes composite coating for selective extraction of fluoroquinolones in aqueous samples. Analytica Chimica Acta, 2012, 727, 26-33.	2.6	119

#	Article	IF	CITATIONS
361	Nano-cubic structured titanium nitride particle films as cathodes for the effective electrocatalytic debromination of BDE-47. Journal of Hazardous Materials, 2012, 231-232, 105-113.	6.5	37
362	Combined effects of enrichment procedure and non-fermentable or fermentable co-substrate on performance and bacterial community for pentachlorophenol degradation in microbial fuel cells. Bioresource Technology, 2012, 120, 120-126.	4.8	50
363	Capture of double-stranded DNA in stacked-graphene: giving new insight into the graphene/DNA interaction. Chemical Communications, 2012, 48, 564-566.	2.2	46
364	Integrating Plasmonic Nanoparticles with TiO ₂ Photonic Crystal for Enhancement of Visible-Light-Driven Photocatalysis. Environmental Science & Technology, 2012, 46, 1724-1730.	4.6	227
365	Characterisation of acute toxicity, genotoxicity and oxidative stress posed by textile effluent on zebrafish. Journal of Environmental Sciences, 2012, 24, 2019-2027.	3.2	95
366	Visible-light-driven photocatalytic and photoelectrocatalytic debromination of BDE-47 on a macroporous silicon/graphene heterostructure. Separation and Purification Technology, 2012, 96, 154-160.	3.9	23
367	g-C3N4/TiO2 hybrid photocatalyst with wide absorption wavelength range and effective photogenerated charge separation. Separation and Purification Technology, 2012, 99, 50-54.	3.9	211
368	Graphene oxide modified g-C ₃ N ₄ hybrid with enhanced photocatalytic capability under visible light irradiation. Journal of Materials Chemistry, 2012, 22, 2721-2726.	6.7	687
369	Graphene-TiO2 Composite Photocatalyst with Enhanced Photocatalytic Performance. Chinese Journal of Catalysis, 2012, 33, 777-782.	6.9	28
370	Photochemical synthesis of highly fluorescent CdTe quantum dots for "on–off–on―detection of Cu(II) ions. Inorganica Chimica Acta, 2012, 392, 236-240.	1.2	13
371	Competitive adsorption and desorption of copper and lead in some soil of North China. Frontiers of Environmental Science and Engineering, 2012, 6, 484-492.	3.3	18
372	Response to the comments on the paper "Bioaugmentation and functional partitioning in a zero valent iron-anaerobic reactor for sulfate-containing wastewater treatment― Chemical Engineering Journal, 2012, 209, 680-681.	6.6	1
373	Photoelectrochemical immunoassay for microcystin-LR based on a fluorine-doped tin oxide glass electrode modified with a CdS-graphene composite. Mikrochimica Acta, 2012, 179, 163-170.	2.5	39
374	Stimuli-responsive peroxidase mimicking at a smart graphene interface. Chemical Communications, 2012, 48, 7055.	2.2	76
375	Interface Engineering Catalytic Graphene for Smart Colorimetric Biosensing. ACS Nano, 2012, 6, 3142-3151.	7.3	270
376	Mineralization of pentachlorophenol with enhanced degradation and power generation from air cathode microbial fuel cells. Biotechnology and Bioengineering, 2012, 109, 2211-2221.	1.7	47
377	Cold modified microelectrode for direct tetracycline detection. Frontiers of Environmental Science and Engineering, 2012, 6, 313-319.	3.3	23
378	Optimization of anaerobic acidogenesis by adding Fe0 powder to enhance anaerobic wastewater treatment. Chemical Engineering Journal, 2012, 192, 179-185.	6.6	186

#	Article	IF	CITATIONS
379	Selective catalytic oxidation of ammonia to nitrogen over ceria–zirconia mixed oxides. Applied Catalysis A: General, 2012, 411-412, 131-138.	2.2	81
380	An anaerobic reactor packed with a pair of Fe-graphite plate electrodes for bioaugmentation of azo dye wastewater treatment. Biochemical Engineering Journal, 2012, 63, 31-37.	1.8	49
381	Reductive dechlorination and mineralization of pentachlorophenol in biocathode microbial fuel cells. Bioresource Technology, 2012, 111, 167-174.	4.8	112
382	Enhancement of nitrogen removal in a novel anammox reactor packed with Fe electrode. Bioresource Technology, 2012, 114, 102-108.	4.8	83
383	Steady performance of a zero valent iron packed anaerobic reactor for azo dye wastewater treatment under variable influent quality. Journal of Environmental Sciences, 2012, 24, 720-727.	3.2	38
384	Enhanced photocatalytic degradation of tetracycline hydrochloride by molecular imprinted film modified TiO2 nanotubes. Science Bulletin, 2012, 57, 601-605.	1.7	30
385	CeO ₂ –TiO ₂ Coated Ceramic Membrane with Catalytic Ozonation Capability for Treatment of Tetracycline in Drinking Water. Science of Advanced Materials, 2012, 4, 1191-1199.	0.1	32
386	Effects of Surface Features on Sulfur Dioxide Adsorption on Calcined NiAl Hydrotalcite-like Compounds. Environmental Science & Technology, 2011, 45, 5373-5379.	4.6	51
387	TiO2 nanotube/Ag–AgBr three-component nanojunction for efficient photoconversion. Journal of Materials Chemistry, 2011, 21, 18067.	6.7	89
388	Salt-controlled assembly of stacked-graphene for capturing fluorescence and its application in chemical genotoxicity screening. Journal of Materials Chemistry, 2011, 21, 15266.	6.7	6
389	Enhanced Adsorption of PFOA and PFOS on Multiwalled Carbon Nanotubes under Electrochemical Assistance. Environmental Science & amp; Technology, 2011, 45, 8498-8505.	4.6	152
390	Fabrication of a TiO2/Au Nanorod Array for Enhanced Photocatalysis. Chinese Journal of Catalysis, 2011, 32, 1838-1843.	6.9	8
391	Label-free fluorescent detection of Cu(ii) ions based on DNA cleavage-dependent graphene-quenched DNAzymes. Chemical Communications, 2011, 47, 7749.	2.2	82
392	Controllable oxidative DNA cleavage-dependent regulation of graphene/DNA interaction. Chemical Communications, 2011, 47, 4084.	2.2	50
393	Graphene Sheets Grafted Ag@AgCl Hybrid with Enhanced Plasmonic Photocatalytic Activity under Visible Light. Environmental Science & Technology, 2011, 45, 5731-5736.	4.6	393
394	Phytotoxicity of PFOS and PFOA to Brassica chinensis in different Chinese soils. Ecotoxicology and Environmental Safety, 2011, 74, 1343-1347.	2.9	45
395	Applying an electric field in a built-in zero valent iron–ÂAnaerobic reactor for enhancement of sludge granulation. Water Research, 2011, 45, 1258-1266.	5.3	141
396	In situ controllable growth of noble metal nanodot on graphene sheet. Journal of Materials Chemistry, 2011, 21, 12986.	6.7	36

XIE QUAN

#	Article	IF	CITATIONS
397	Selective detection of nanomolar Cr(<scp>vi</scp>) in aqueous solution based on 1,4-dithiothreitol functionalized gold nanoparticles. Analytical Methods, 2011, 3, 343-347.	1.3	50
398	In-situ synthesis of Ag/SBA-15 nanocomposites by the "pH-adjusting―method. Materials Letters, 2011, 65, 1892-1895.	1.3	35
399	Effects of Cu(II) and humic acid on atrazine photodegradation. Journal of Environmental Sciences, 2011, 23, 773-777.	3.2	26
400	Low temperature CO oxidation over Ag/SBA-15 nanocomposites prepared via in-situ "pH-adjusting― method. Catalysis Communications, 2011, 16, 11-14.	1.6	36
401	Bioaugmentation and functional partitioning in a zero valent iron-anaerobic reactor for sulfate-containing wastewater treatment. Chemical Engineering Journal, 2011, 174, 159-165.	6.6	98
402	Catalytic oxidation of toluene over manganese oxide octahedral molecular sieves (OMS-2) synthesized by different methods. Chemical Engineering Journal, 2011, 178, 191-196.	6.6	67
403	Formation of 2′-hydroxy-2,3′,4,5′-tetrabromodipheyl ether (2′-HO-BDE68) from 2,4-dibromophenol in aqueous solution under simulated sunlight irradiation. Chemosphere, 2011, 84, 512-518.	4.2	26
404	Constructing graphene/InNbO4 composite with excellent adsorptivity and charge separation performance for enhanced visible-light-driven photocatalytic ability. Applied Catalysis B: Environmental, 2011, 105, 237-242.	10.8	79
405	Effects of an electric field and zero valent iron on anaerobic treatment of azo dye wastewater and microbial community structures. Bioresource Technology, 2011, 102, 2578-2584.	4.8	74
406	A graphene-based platform for single nucleotide polymorphism (SNP) genotyping. Biosensors and Bioelectronics, 2011, 26, 4213-4216.	5.3	23
407	A "turn-on―fluorescent copper biosensor based on DNA cleavage-dependent graphene-quenched DNAzyme. Biosensors and Bioelectronics, 2011, 26, 4111-4116.	5.3	99
408	Evaluation of a novel microextraction technique for aqueous samples: Porous membrane envelope filled with multiwalled carbon nanotubes coated with molecularly imprinted polymer. Journal of Separation Science, 2011, 34, 707-715.	1.3	31
409	Performance of a ZVI-UASB reactor for azo dye wastewater treatment. Journal of Chemical Technology and Biotechnology, 2011, 86, 199-204.	1.6	75
410	Electrochemical Determination of Tetracycline Using Molecularly Imprinted Polymer Modified Carbon Nanotubeâ€Gold Nanoparticles Electrode. Electroanalysis, 2011, 23, 1863-1869.	1.5	77
411	Remarkable improvement of visible light photocatalysis with PANI modified core–shell mesoporous TiO2 microspheres. Applied Catalysis B: Environmental, 2011, 102, 126-131.	10.8	142
412	Electron transfer mechanisms, new applications, and performance of biocathode microbial fuel cells. Bioresource Technology, 2011, 102, 316-323.	4.8	304
413	Adsorption of ionizable organic contaminants on multi-walled carbon nanotubes with different oxygen contents. Journal of Hazardous Materials, 2011, 186, 407-415.	6.5	142
414	Enhancement of sludge granulation in a zero valence iron packed anaerobic reactor with a hydraulic circulation. Process Biochemistry, 2011, 46, 471-476.	1.8	50

#	Article	IF	CITATIONS
415	Sensitive amperometric determination of chemical oxygen demand using Ti/Sb–SnO2/PbO2 composite electrode. Sensors and Actuators B: Chemical, 2011, 155, 114-119.	4.0	30
416	Influence of Temperature and Oil Content on the Soil/Air Partition Coefficient for Hexachlorobenzene in Oil-Contaminated Rice Paddy Field Soil. Soil and Sediment Contamination, 2011, 20, 221-233.	1.1	1
417	Fabrication and thickness regulation of graphene film electrode by a facile drying method. Proceedings of the Institution of Mechanical Engineers, Part N: Journal of Nanoengineering and Nanosystems, 2011, 225, 71-73.	0.1	0
418	A built-in zero valent iron anaerobic reactor to enhance treatment of azo dye wastewater. Water Science and Technology, 2011, 63, 741-746.	1.2	55
419	Enhancement of hexavalent chromium reduction and electricity production from a biocathode microbial fuel cell. Bioprocess and Biosystems Engineering, 2010, 33, 937-945.	1.7	129
420	Electrocatalytic dechlorination of 2,4,5-trichlorobiphenyl using an aligned carbon nanotubes electrode deposited with palladium nanoparticles. Science Bulletin, 2010, 55, 358-364.	1.7	8
421	Complexation of iron by salicylic acid and its effect on atrazine photodegradation in aqueous solution. Frontiers of Environmental Science and Engineering in China, 2010, 4, 157-163.	0.8	8
422	Electrochemical Method for Synthesis of a ZnFe ₂ O ₄ /TiO ₂ Composite Nanotube Array Modified Electrode with Enhanced Photoelectrochemical Activity. Advanced Functional Materials, 2010, 20, 2165-2174.	7.8	317
423	A Structured Macroporous Silicon/Graphene Heterojunction for Efficient Photoconversion. Angewandte Chemie - International Edition, 2010, 49, 5106-5109.	7.2	76
424	A microbial fuel cell–electroâ€oxidation system for coking wastewater treatment and bioelectricity generation. Journal of Chemical Technology and Biotechnology, 2010, 85, 621-627.	1.6	54
425	Enhanced oxidation of 4-chlorophenol using sulfate radicals generated from zero-valent iron and peroxydisulfate at ambient temperature. Separation and Purification Technology, 2010, 71, 302-307.	3.9	251
426	Studies of silver species for low-temperature CO oxidation on Ag/SiO2 catalysts. Separation and Purification Technology, 2010, 72, 395-400.	3.9	93
427	Enhanced photocatalytic activity for titanium dioxide by co-modifying with silica and fluorine. Journal of Hazardous Materials, 2010, 175, 258-266.	6.5	26
428	Effect of Si doping on photoelectrocatalytic decomposition of phenol of BiVO4 film under visible light. Journal of Hazardous Materials, 2010, 177, 914-917.	6.5	57
429	Experimental and modeling study of selective catalytic reduction of NOx with NH3 over wire mesh honeycomb catalysts. Chemical Engineering Journal, 2010, 165, 769-775.	6.6	24
430	Electrochemically assisted photocatalytic degradation of phenol using silicon-doped TiO2 nanofilm electrode. Desalination, 2010, 252, 143-148.	4.0	28
431	New Photocatalyst Electrodes and Their Photocatalytic Degradation Properties of Organics. Current Organic Chemistry, 2010, 14, 709-727.	0.9	4
432	Distance-independent quenching of quantum dots by nanoscale-graphene in self-assembled sandwich immunoassay. Chemical Communications, 2010, 46, 7909.	2.2	106

#	Article	IF	CITATIONS
433	Photochlorination of bisphenol A by UV-Vis light irradiation in saline solution: effects of iron, nitrate and citric acid. Environmental Chemistry, 2010, 7, 548.	0.7	9
434	Electrochemically Assisted Photocatalytic Degradation of 4-Chlorophenol by ZnFe ₂ O ₄ â^Modified TiO ₂ Nanotube Array Electrode under Visible Light Irradiation. Environmental Science & Technology, 2010, 44, 5098-5103.	4.6	176
435	Photochemical Effect of Humic Acid Components Separated Using Molecular Imprinting Method Applying Porphyrin-like Substances as Templates in Aqueous Solution. Environmental Science & Technology, 2010, 44, 5812-5817.	4.6	23
436	Structuring a TiO ₂ -Based Photonic Crystal Photocatalyst with Schottky Junction for Efficient Photocatalysis. Environmental Science & Technology, 2010, 44, 451-455.	4.6	75
437	Highly sensitive and selective fluorescence sensor based on functional SBA-15 for detection of Hg2+ in Aqueous Media. Talanta, 2010, 81, 643-649.	2.9	79
438	Performing a microfiltration integrated with photocatalysis using an Ag-TiO2/HAP/Al2O3 composite membrane for water treatment: Evaluating effectiveness for humic acid removal and anti-fouling properties. Water Research, 2010, 44, 6104-6114.	5.3	109
439	Determination and prediction of octanol–air partition coefficients of hydroxylated and methoxylated polybrominated diphenyl ethers. Chemosphere, 2010, 80, 660-664.	4.2	13
440	Photonic Crystal Coupled TiO ₂ /Polymer Hybrid for Efficient Photocatalysis under Visible Light Irradiation. Environmental Science & Technology, 2010, 44, 3481-3485.	4.6	121
441	Signal amplification via cation exchange reaction: an example in the ratiometric fluorescence probe for ultrasensitive and selective sensing of Cu(ii). Chemical Communications, 2010, 46, 1144-1146.	2.2	41
442	Microwave thermal remediation of crude oil contaminated soil enhanced by carbon fiber. Journal of Environmental Sciences, 2009, 21, 1290-1295.	3.2	69
443	Photo-oxidation of gas-phase cyclohexane species over nanostructured TiO2 fabricated by different strategies. Separation and Purification Technology, 2009, 67, 326-330.	3.9	11
444	Facile fabrication, characterization, and enhanced photoelectrocatalytic degradation performance of highly oriented TiO2 nanotube arrays. Journal of Nanoparticle Research, 2009, 11, 2153-2162.	0.8	29
445	Contribution of black carbon to nonlinearity of sorption and desorption of acetochlor on sediment. Frontiers of Environmental Science and Engineering in China, 2009, 3, 69-74.	0.8	6
446	Removal of multicomponent VOCs in off-gases from an oil refining wastewater treatment plant by a compost-based biofilter system. Frontiers of Environmental Science and Engineering in China, 2009, 3, 483-491.	0.8	1
447	Integration of separation and photocatalysis using an inorganic membrane modified with Si-doped TiO2 for water purification. Journal of Membrane Science, 2009, 335, 58-67.	4.1	84
448	Visible light photoelectrocatalysis with salicylic acid-modified TiO2 nanotube array electrode for p-nitrophenol degradation. Journal of Hazardous Materials, 2009, 166, 547-552.	6.5	52
449	Preparation of Ag doped BiVO4 film and its enhanced photoelectrocatalytic (PEC) ability of phenol degradation under visible light. Journal of Hazardous Materials, 2009, 167, 911-914.	6.5	96
450	Ag–TiO2/HAP/Al2O3 bioceramic composite membrane: Fabrication, characterization and bactericidal activity. Journal of Membrane Science, 2009, 336, 109-117.	4.1	96

XIE QUAN

#	Article	IF	CITATIONS
451	Preparation and characterization of BiVO4 film electrode and investigation of its photoelectrocatalytic (PEC) ability under visible light. Separation and Purification Technology, 2009, 64, 309-313.	3.9	36
452	Photoelectrochemical characterization and application of direct-grown nanostructured anatase film via hydrothermal reactions. Separation and Purification Technology, 2009, 68, 255-260.	3.9	4
453	Evaluation of bias potential enhanced photocatalytic degradation of 4-chlorophenol with TiO2 nanotube fabricated by anodic oxidation method. Chemical Engineering Journal, 2009, 146, 30-35.	6.6	131
454	Rapid startup of a hybrid UASB-AFF reactor using bi-circulation. Chemical Engineering Journal, 2009, 155, 266-271.	6.6	35
455	Preparation and evaluation of molecularly imprinted solid-phase microextraction fibers for selective extraction of bisphenol A in complex samples. Journal of Chromatography A, 2009, 1216, 5647-5654.	1.8	90
456	Structural and photovoltaic properties of highly ordered ZnFe2O4 nanotube arrays fabricated by a facile sol–gel template method. Acta Materialia, 2009, 57, 2684-2690.	3.8	84
457	Silicon nanowire/TiO2 heterojunction arrays for effective photoelectrocatalysis under simulated solar light irradiation. Applied Catalysis B: Environmental, 2009, 90, 242-248.	10.8	65
458	Effective Utilization of Visible Light (Including λ > 600 nm) in Phenol Degradation with p-Silicon Nanowire/TiO ₂ Core/Shell Heterojunction Array Cathode. Environmental Science & Technology, 2009, 43, 7849-7855.	4.6	35
459	"Mulberry-like―CdSe Nanoclusters Anchored on TiO ₂ Nanotube Arrays: A Novel Architecture with Remarkable Photoelectrochemical Performance. Chemistry of Materials, 2009, 21, 3090-3095.	3.2	105
460	Separation of Phthalocyanine-like Substances from Humic Acids Using a Molecular Imprinting Method and Their Photochemical Activity under Simulated Sunlight Irradiation. Journal of Agricultural and Food Chemistry, 2009, 57, 6927-6931.	2.4	15
461	Perfluorosulfonates and perfluorocarboxylates in snow and rain in Dalian, China. Environment International, 2009, 35, 737-742.	4.8	57
462	Effect of perfluorooctane sulfonate on toxicity and cell uptake of other compounds with different hydrophobicity in green alga. Chemosphere, 2009, 75, 405-409.	4.2	37
463	Temperature-dependence of soil/air partition coefficients for selected polycyclic aromatic hydrocarbons and organochlorine pesticides over a temperature range of â~'30 to +30°C. Chemosphere, 2009, 76, 465-471.	4.2	22
464	Evaluating the fate of three HCHs in the typically agricultural environment of Liaoning Province, China. Chemosphere, 2009, 76, 792-798.	4.2	4
465	Temperature-dependence of soil/air partition coefficient for polychlorinated biphenyls at subzero temperatures. Chemosphere, 2009, 77, 1427-1433.	4.2	9
466	Sorption of perfluorooctane sulfonate (PFOS) on oil and oil-derived black carbon: Influence of solution pH and [Ca2+]. Chemosphere, 2009, 77, 1406-1411.	4.2	66
467	Photochemical activity and characterization of the complex of humic acids with iron(III). Journal of Geochemical Exploration, 2009, 102, 49-55.	1.5	55
468	Flow Injection Analysis of Chemical Oxygen Demand (COD) by Using a Boron-Doped Diamond (BDD) Electrode. Environmental Science & Technology, 2009, 43, 1935-1939.	4.6	67

#	Article	IF	CITATIONS
469	Formation of Chlorinated Intermediate from Bisphenol A in Surface Saline Water under Simulated Solar Light Irradiation. Environmental Science & Technology, 2009, 43, 7712-7717.	4.6	68
470	Highly sensitive fluorescence probe based on functional SBA-15 for selective detection of Hg ²⁺ in aqueous media. Journal of Environmental Monitoring, 2009, 11, 648-653.	2.1	52
471	Importance of Environmental Black Carbon to Dissolved Petroleum Hydrocarbons Sorption on Soil. Soil and Sediment Contamination, 2009, 18, 184-194.	1.1	2
472	Photoeletrocatalytic Activity of a Cu ₂ O-Loaded Self-Organized Highly Oriented TiO ₂ Nanotube Array Electrode for 4-Chlorophenol Degradation. Environmental Science & Technology, 2009, 43, 858-863.	4.6	236
473	Integrated electrochemically enhanced adsorption with electrochemical regeneration for removal of acid orange 7 using activated carbon fibers. Separation and Purification Technology, 2008, 59, 43-49.	3.9	45
474	Characterization of boron-doped TiO2 nanotube arrays prepared by electrochemical method and its visible light activity. Separation and Purification Technology, 2008, 62, 668-673.	3.9	112
475	Investigation of Pentachlorophenol Vertical Transportation in Soil Column During its Phototransformation on the Soil Surface. Water, Air, and Soil Pollution, 2008, 189, 103-112.	1.1	2
476	Effects of humic acid fractions with different polarities on photodegradation of 2,4-D in aqueous environments. Frontiers of Environmental Science and Engineering in China, 2008, 2, 291-296.	0.8	8
477	Photoelectrochemical Manifestation of Photoelectron Transport Properties of Vertically Aligned Nanotubular TiO ₂ Photoanodes. ChemPhysChem, 2008, 9, 117-123.	1.0	39
478	Synthesis of molecular imprinted polymer modified TiO2 nanotube array electrode and their photoelectrocatalytic activity. Journal of Solid State Chemistry, 2008, 181, 2852-2858.	1.4	57
479	Treatment of petroleum refinery wastewater by microwave-assisted catalytic wet air oxidation under low temperature and low pressure. Separation and Purification Technology, 2008, 62, 565-570.	3.9	95
480	Controllable synthesis of ZnO nanoflowers and their morphology-dependent photocatalytic activities. Separation and Purification Technology, 2008, 62, 727-732.	3.9	291
481	Photocatalytic reaction by Fe(III)–citrate complex and its effect on the photodegradation of atrazine in aqueous solution. Journal of Photochemistry and Photobiology A: Chemistry, 2008, 197, 382-388.	2.0	108
482	TiO2–carbon nanotube heterojunction arrays with a controllable thickness of TiO2 layer and their first application in photocatalysis. Journal of Photochemistry and Photobiology A: Chemistry, 2008, 200, 301-306.	2.0	123
483	Preparation and characteristics of carbon-supported platinum catalyst and its application in the removal of phenolic pollutants in aqueous solution by microwave-assisted catalytic oxidation. Journal of Hazardous Materials, 2008, 157, 179-186.	6.5	38
484	Electrocatalytic hydrodehalogenation of pentachlorophenol at palladized multiwalled carbon nanotubes electrode. Applied Catalysis B: Environmental, 2008, 80, 122-128.	10.8	66
485	Enhanced generation of oxidative species and phenol degradation in a discharge plasma system coupled with TiO2 photocatalysis. Applied Catalysis B: Environmental, 2008, 83, 72-77.	10.8	100
486	Fabrication of a TiO2/carbon nanowall heterojunction and its photocatalytic ability. Carbon, 2008, 46, 1126-1132.	5.4	93

#	Article	IF	CITATIONS
487	Wire-mesh honeycomb catalyst for selective catalytic reduction of NOx under lean-burn conditions. Catalysis Today, 2008, 139, 130-134.	2.2	23
488	A silicon-doped TiO2 nanotube arrays electrode with enhanced photoelectrocatalytic activity. Applied Surface Science, 2008, 255, 2167-2172.	3.1	91
489	Toxic effect of serial perfluorosulfonic and perfluorocarboxylic acids on the membrane system of a freshwater alga measured by flow cytometry. Environmental Toxicology and Chemistry, 2008, 27, 1597-1604.	2.2	72
490	Solubility and sorption of petroleum hydrocarbons in water and cosolvent systems. Journal of Environmental Sciences, 2008, 20, 1177-1182.	3.2	9
491	Highly Oriented 1-D ZnO Nanorod Arrays on Zinc Foil:  Direct Growth from Substrate, Optical Properties and Photocatalytic Activities. Journal of Physical Chemistry C, 2008, 112, 7332-7336.	1.5	125
492	Electrochemically Assisted Photocatalytic Inactivation of Escherichia coli under Visible Light Using a ZnIn ₂ S ₄ Film Electrode. Langmuir, 2008, 24, 7599-7604.	1.6	91
493	Fabrication of TiO ₂ â^'Pt Coaxial Nanotube Array Schottky Structures for Enhanced Photocatalytic Degradation of Phenol in Aqueous Solution. Journal of Physical Chemistry C, 2008, 112, 9285-9290.	1.5	128
494	Ecotoxicological characterization of photoelectrocatalytic process for degradation of pentachlorophenol on titania nanotubes electrode. Ecotoxicology and Environmental Safety, 2008, 71, 267-273.	2.9	8
495	Photoinductive activity of humic acid fractions with the presence of Fe(III): The role of aromaticity and oxygen groups involved in fractions. Chemosphere, 2008, 72, 925-931.	4.2	29
496	Sorption of polar and nonpolar organic contaminants by oil-contaminated soil. Chemosphere, 2008, 73, 1832-1837.	4.2	20
497	Facile Method for Fabricating Boron-Doped TiO ₂ Nanotube Array with Enhanced Photoelectrocatalytic Properties. Industrial & Engineering Chemistry Research, 2008, 47, 3804-3808.	1.8	107
498	Microwave-Induced Thermal Treatment of Petroleum Hydrocarbon-Contaminated Soil. Soil and Sediment Contamination, 2008, 17, 486-496.	1.1	10
499	Fabrication of a TiO ₂ â^BDD Heterojunction and its Application As a Photocatalyst for the Simultaneous Oxidation of an Azo Dye and Reduction of Cr(VI). Environmental Science & Technology, 2008, 42, 3791-3796.	4.6	121
500	Direct growth and photoelectrochemical properties of tungsten oxide nanobelt arrays. Nanotechnology, 2008, 19, 065704.	1.3	35
501	Enhanced Photodegradation of PNP on Soil Surface under UV Irradiation with TiO2. Soil and Sediment Contamination, 2007, 16, 413-421.	1.1	16
502	Fabrication of nanomaterial models and their applications in water treatment. , 2007, , .		1
503	Medium-Strength Ammonium Removal Using a Two-Stage Moving Bed Biofilm Reactor System. Environmental Engineering Science, 2007, 24, 595-601.	0.8	9
504	Photoelectrocatalytic degradation of pentachlorophenol in aqueous solution using a TiO2 nanotube film electrode. Environmental Pollution, 2007, 147, 409-414.	3.7	122

#	Article	IF	CITATIONS
505	Long-term fate of three hexachlorocyclohexanes in the lower reach of Liao River basin: Dynamic mass budgets and pathways. Chemosphere, 2007, 69, 1159-1165.	4.2	10
506	TiO ₂ â^'Multiwalled Carbon Nanotube Heterojunction Arrays and Their Charge Separation Capability. Journal of Physical Chemistry C, 2007, 111, 12987-12991.	1.5	222
507	High Photocatalytic Capability of Self-Assembled Nanoporous WO3with Preferential Orientation of (002) Planes. Environmental Science & amp; Technology, 2007, 41, 4422-4427.	4.6	202
508	Fabrication of Boron-Doped TiO ₂ Nanotube Array Electrode and Investigation of Its Photoelectrochemical Capability. Journal of Physical Chemistry C, 2007, 111, 11836-11842.	1.5	271
509	Atrazine Photodegradation in Aqueous Solution Induced by Interaction of Humic Acids and Iron: Photoformation of Iron(II) and Hydrogen Peroxide. Journal of Agricultural and Food Chemistry, 2007, 55, 8650-8656.	2.4	36
510	Preparation of well-adhered γ-Al2O3 washcoat on metallic wire mesh monoliths by electrophoretic deposition. Applied Surface Science, 2007, 253, 3303-3310.	3.1	39
511	Electrochemical enhancement of adsorption capacity of activated carbon fibers and their surface physicochemical characterizations. Electrochimica Acta, 2007, 52, 3075-3081.	2.6	50
512	Amperometric determination of chemical oxygen demand using boron-doped diamond (BDD) sensor. Electrochemistry Communications, 2007, 9, 2280-2285.	2.3	61
513	Generation of hydroxyl radical in aqueous solution by microwave energy using activated carbon as catalyst and its potential in removal of persistent organic substances. Journal of Molecular Catalysis A, 2007, 263, 216-222.	4.8	90
514	Formation of hydrogen peroxide and degradation of phenol in synergistic system of pulsed corona discharge combined with TiO2 photocatalysis. Journal of Hazardous Materials, 2007, 141, 336-343.	6.5	87
515	Photocatalytic remediation of γ-hexachlorocyclohexane contaminated soils using TiO2 and montmorillonite composite photocatalyst. Journal of Environmental Sciences, 2007, 19, 358-361.	3.2	22
516	Catalytic reductive dechlorination of p-chlorophenol in water using Ni/Fe nanoscale particles. Journal of Environmental Sciences, 2007, 19, 362-366.	3.2	44
517	Fabrication of needle-like ZnO nanorods arrays by a low-temperature seed-layer growth approach in solution. Applied Physics A: Materials Science and Processing, 2007, 89, 673-679.	1.1	11
518	Kinetics of enhanced adsorption by polarization for organic pollutants on activated carbon fiber. Frontiers of Environmental Science and Engineering in China, 2007, 1, 83-88.	0.8	13
519	Dynamic fate modeling of γ-hexachlorocyclohexane in the lower reaches of the Liao River. Frontiers of Environmental Science and Engineering in China, 2007, 1, 166-171.	0.8	0
520	Preparation of Zn-doped TiO2 nanotubes electrode and its application in pentachlorophenol photoelectrocatalytic degradation. Science Bulletin, 2007, 52, 1456-1461.	1.7	52
521	Fabrication and Characterization of Silica/Titania Nanotubes Composite Membrane with Photocatalytic Capability. Environmental Science & Technology, 2006, 40, 6104-6109.	4.6	124
522	Photoelectrocatalytic treatment of pentachlorophenol in aqueous solution using a rutile nanotube-like TiO2/Ti electrode. Photochemical and Photobiological Sciences, 2006, 5, 808.	1.6	20

#	Article	IF	CITATIONS
523	Complexes of fulvic acid on the surface of hematite, goethite, and akaganeite: FTIR observation. Chemosphere, 2006, 63, 403-410.	4.2	158
524	Rapid and complete dechlorination of PCP in aqueous solution using Ni–Fe nanoparticles under assistance of ultrasound. Chemosphere, 2006, 65, 58-64.	4.2	77
525	Degradation of p-nitrophenol in aqueous solution by microwave assisted oxidation process through a granular activated carbon fixed bed. Water Research, 2006, 40, 3061-3068.	5.3	114
526	Long-term operation of a compost-based biofilter for biological removal of n-butyl acetate, p-xylene and ammonia gas from an air stream. Biochemical Engineering Journal, 2006, 32, 84-92.	1.8	28
527	Decoloration of azo dye by a multi-needle-to-plate high-voltage pulsed corona discharge system in water. Journal of Electrostatics, 2006, 64, 416-421.	1.0	126
528	The removal of sodium dodecylbenzene sulfonate surfactant from water using silica/titania nanorods/nanotubes composite membrane with photocatalytic capability. Applied Surface Science, 2006, 252, 8598-8604.	3.1	49
529	Fabrication of photocatalytic membrane and evaluation its efficiency in removal of organic pollutants from water. Separation and Purification Technology, 2006, 50, 147-155.	3.9	113
530	Electrochemically enhanced adsorption of aniline on activated carbon fibers. Separation and Purification Technology, 2006, 50, 365-372.	3.9	93
531	Removal of p-xylene from an air stream in a hybrid biofilter. Journal of Hazardous Materials, 2006, 136, 288-295.	6.5	41
532	Microwave assisted catalytic wet air oxidation of H-acid in aqueous solution under the atmospheric pressure using activated carbon as catalyst. Journal of Hazardous Materials, 2006, 137, 534-540.	6.5	37
533	Electrochemically enhanced adsorption of phenol on activated carbon fibers in basic aqueous solution. Journal of Colloid and Interface Science, 2006, 299, 766-771.	5.0	48
534	Preparation and characterization of aligned carbon nanotubes coated with titania nanoparticles. Science Bulletin, 2006, 51, 2294-2296.	1.7	14
535	Enhanced photodegradation of phenolic compounds by adding TiO2 to soil in a rotary reactor. Journal of Environmental Sciences, 2006, 18, 1107-1112.	3.2	5
536	Removal of ternary VOCs in air streams at high loads using a compost-based biofilter. Biochemical Engineering Journal, 2005, 23, 85-95.	1.8	35
537	Photodegradation of Î ³ -HCH by α-Fe2O3 and the influence of fulvic acid. Journal of Photochemistry and Photobiology A: Chemistry, 2005, 173, 143-149.	2.0	27
538	Adsorption and electrocatalytic dechlorination of pentachlorophenol on palladium-loaded activated carbon fibers. Separation and Purification Technology, 2005, 47, 73-79.	3.9	40
539	Bioavailability of zinc in the sediment to the estuarine amphipod Grandidierella japonica. Hydrobiologia, 2005, 541, 149-154.	1.0	17
540	Preparation of Titania Nanotubes and Their Environmental Applications as Electrode. Environmental Science & Technology, 2005, 39, 3770-3775.	4.6	414

#	Article	IF	CITATIONS
541	Enhancement of p,pâ \in^2 -DDT photodegradation on soil surfaces using TiO2 induced by UV-light. Chemosphere, 2005, 60, 266-273.	4.2	80
542	Degradation of H-acid in aqueous solution by microwave assisted wet air oxidation using Ni-loaded GAC as catalyst. Journal of Environmental Sciences, 2005, 17, 433-6.	3.2	5
543	The role of UV-B on the degradation of PCDD/Fs and PAHs sorbed on surfaces of spruce (Picea abies (L.)) Tj ETQq1	1 0.7843 3.9	14 rgBT /0\ 32
544	Synthesis and photocatalytic properties of quantum confined titanium dioxide nanoparticle. Scripta Materialia, 2004, 50, 499-505.	2.6	48
545	Synergetic degradation of 2,4-D by integrated photo- and electrochemical catalysis on a Pt doped TiO2/Ti electrode. Separation and Purification Technology, 2004, 34, 73-79.	3.9	52
546	Effect of embedded-silica on microstructure and photocatalytic activity of titania prepared by ultrasound-assisted hydrolysis. Applied Catalysis B: Environmental, 2004, 52, 33-40.	10.8	64
547	Complexes of Fulvic Acid on Hematite Interfaces: Characterization and Photochemical Properties. Journal of Applied Spectroscopy, 2004, 71, 721-730.	0.3	2
548	UNIVERSAL PREDICTIVE MODELS ON OCTANOL–AIR PARTITION COEFFICIENTS AT DIFFERENT TEMPERATURES FOR PERSISTENT ORGANIC POLLUTANTS. Environmental Toxicology and Chemistry, 2004, 23, 2309.	2.2	34
549	Comparison of different extraction techniques for the determination of chlorinated pesticides in animal feed. Analytical and Bioanalytical Chemistry, 2004, 378, 1861-1867.	1.9	36
550	Different effects of humic substances on photodegradation of p,p′-DDT on soil surfaces in the presence of TiO2 under UV and visible light. Journal of Photochemistry and Photobiology A: Chemistry, 2004, 167, 177-183.	2.0	43
551	Temperature measurement of GAC and decomposition of PCP loaded on GAC and GAC-supported copper catalyst in microwave irradiation. Applied Catalysis A: General, 2004, 264, 53-58.	2.2	74
552	Simultaneous pentachlorophenol decomposition and granular activated carbon regeneration assisted by microwave irradiation. Carbon, 2004, 42, 415-422.	5.4	171
553	Photoinduced Transformation of γ-HCH in the Presence of Dissolved Organic Matter and Enhanced Photoreactive Activity of Humate-Coated α-Fe2O3. Langmuir, 2004, 20, 4867-4873.	1.6	29
554	Regeneration of acid orange 7-exhausted granular activated carbons with microwave irradiation. Water Research, 2004, 38, 4484-4490.	5.3	87
555	The role of UV-B on the degradation of PCDD/Fs and PAHs sorbed on surfaces of spruce (Picea abies (L.)) Tj ETQq1	1.9.7843 3.9	14 rgBT /0
556	Quantitative structure-property relationships for octanol–air partition coefficients of polychlorinated naphthalenes, chlorobenzenes and p,pâ€2-DDT. Computational Biology and Chemistry, 2003, 27, 165-171.	1.1	25
557	Photodegradation of PCDD/Fs adsorbed on spruce (Picea abies (L.) Karst.) needles under sunlight irradiation. Chemosphere, 2003, 50, 1217-1225.	4.2	56
558	Effects of Fe2O3, organic matter and carbonate on photocatalytic degradation of lindane in the sediment from the Liao River. China. Chemosphere, 2003, 52, 1749-1755.	4.2	22

#	Article	IF	CITATIONS
559	Photolysis of polycyclic aromatic hydrocarbons adsorbed on spruce [Picea abies (L.) Karst.] needles under sunlight irradiation. Environmental Pollution, 2003, 123, 39-45.	3.7	83
560	Triazines in the aquatic systems of the Eastern Chinese Rivers Liao-He and Yangtse. Chemosphere, 2002, 47, 455-466.	4.2	38
561	Quantitative structure–property relationships for octanol–air partition coefficients of polychlorinated biphenyls. Chemosphere, 2002, 48, 535-544.	4.2	61
562	Occurrence of triazines in surface and drinking water of Liaoning Province in Eastern China. Journal of Proteomics, 2002, 53, 217-228.	2.4	39
563	Simultaneous determination of chlorinated organic compounds from environmental samples using gas chromatography coupled with a micro electron capture detector and micro-plasma atomic emission detector. Spectrochimica Acta, Part B: Atomic Spectroscopy, 2002, 57, 189-199.	1.5	22
564	Simultaneous removal of ethyl acetate and toluene in air streams using compost-based biofilters. Journal of Hazardous Materials, 2002, 95, 199-213.	6.5	52
565	Toluene vapour degradation and microbial community in biofilter at various moisture content. Process Biochemistry, 2002, 38, 109-113.	1.8	37
566	Is it possible to develop a QSPR model for direct photolysis half-lives of PAHs under irradiation of sunlight?. Environmental Pollution, 2001, 114, 137-143.	3.7	53
567	Quantitative structure–property relationship studies on direct photolysis of selected polycyclic aromatic hydrocarbons in atmospheric aerosol. Chemosphere, 2001, 42, 263-270.	4.2	41
568	Quantitative structure–property relationships (QSPRs) on direct photolysis quantum yields of PCDDs. Chemosphere, 2001, 43, 235-241.	4.2	35
569	Quantitative structure–property relationship studies on n-octanol/water partitioning coefficients of PCDD/Fs. Chemosphere, 2001, 44, 1369-1374.	4.2	42
570	Quantitative structure–property relationship study on reductive dehalogenation of selected halogenated aliphatic hydrocarbons in sediment slurries. Chemosphere, 2001, 44, 1557-1563.	4.2	15
571	Quantitative structure–property relationships (QSPRs) on direct photolysis of PCDDs. Chemosphere, 2001, 45, 151-159.	4.2	14
572	Quantitative structure–property relationships on photodegradation of PCDD/Fs in cuticular waxes of laurel cherry (Prunus laurocerasus). Science of the Total Environment, 2001, 269, 163-170.	3.9	24
573	Long-term results of ammonia removal and transformation by biofiltration. Journal of Hazardous Materials, 2000, 80, 259-269.	6.5	67
574	The use of PLS algorithms and quantum chemical parameters derived from PM3 hamiltonian in QSPR studies on direct photolysis quantum yields of substituted aromatic halides. Chemosphere, 2000, 40, 1319-1326.	4.2	14
575	Quantitative structure–property relationships for direct photolysis quantum yields of selected polycyclic aromatic hydrocarbons. Science of the Total Environment, 2000, 246, 11-20.	3.9	34
576	The application of quantum chemical and statistical technique in developing quantitative structure-property relationships for the photohydrolysis quantum yields of substituted aromatic halides. Chemosphere, 1998, 37, 1169-1186.	4.2	34

#	Article	IF	CITATIONS
577	Role of Nitrite Ions and Natural Organic Matters as Photosensitizers on Photolysis of Phenol. Advanced Materials Research, 0, 926-930, 226-229.	0.3	1
578	Using ammonia as an additive to fabricate a high performance PVDF hollow membrane for distillation. , 0, 70, 79-85.		0